IEC TR 63141

Edition 1.0 2020-04

TECHNICAL REPORT

colour inside

Damp heat, steady state (unsaturated pressurized vapour with air)

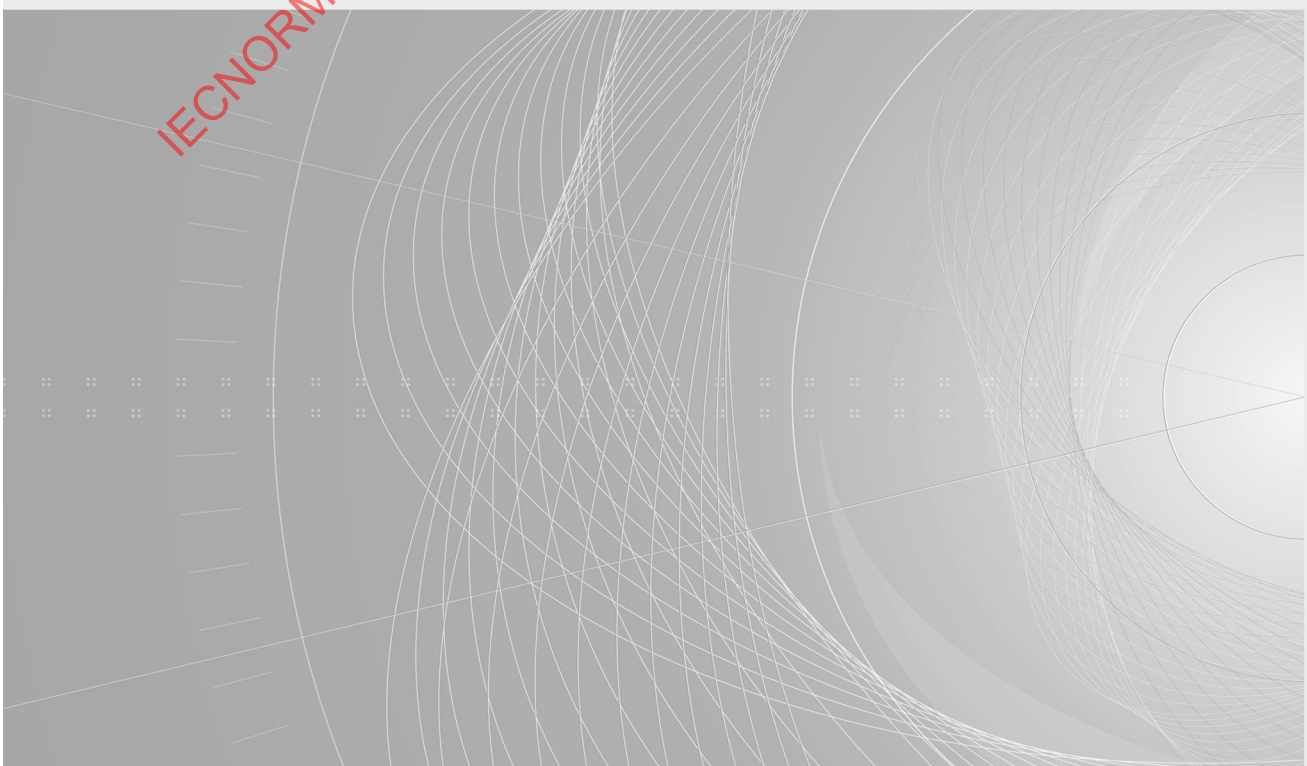

IEC TR 63141:2020-04(en)

IEC Central Office
3, rue de Varembé
CH-1211 Geneva 20
Switzerland

Tel.: +41 22 919 02 11
info@iec.ch
www.iec.ch

About the IEC
The International Electrotechnical Commission (IEC) is the leading global organization that prepares and publishes International Standards for all electrical, electronic and related technologies.

About IEC publications
The technical content of IEC publications is kept under constant review by the IEC. Please make sure that you have the latest edition, a corrigendum or an amendment might have been published.

IEC publications search - webstore.iec.ch/advsearchform
The advanced search enables to find IEC publications by a variety of criteria (reference number, text, technical committee,…). It also gives information on projects, replaced and withdrawn publications.

IEC Just Published - webstore.iec.ch/justpublished
Stay up to date on all new IEC publications. Just Published details all new publications released. Available online and once a month by email.

IEC Customer Service Centre - webstore.iec.ch/csc
If you wish to give us your feedback on this publication or need further assistance, please contact the Customer Service Centre: sales@iec.ch.

Electropedia - www.electropedia.org
The world's leading online dictionary on electrotechnology, containing more than 22 000 terminological entries in English and French, with equivalent terms in 16 additional languages. Also known as the International Electrotechnical Vocabulary (IEV) online.

IEC Glossary - std.iec.ch/glossary
67 000 electrotechnical terminology entries in English and French extracted from the Terms and Definitions clause of IEC publications issued since 2002. Some entries have been collected from earlier publications of IEC TC 37, 77, 86 and CISPR.

IEC TR 63141

Edition 1.0 2020-04

TECHNICAL REPORT

colour inside

Damp heat, steady state (unsaturated pressurized vapour with air)

INTERNATIONAL
ELECTROTECHNICAL
COMMISSION

ICS 19.040

ISBN 978-2-8322-8090-4

Warning! Make sure that you obtained this publication from an authorized distributor.

CONTENTS

INTERNATIONAL ELECTROTECHNICAL COMMISSION

_____

DAMP HEAT, STEADY STATE (UNSATURATED PRESSURIZED VAPOUR WITH AIR)

FOREWORD

1) The International Electrotechnical Commission (IEC) is a worldwide organization for standardization comprising all national electrotechnical committees (IEC National Committees). The object of IEC is to promote international co-operation on all questions concerning standardization in the electrical and electronic fields. To this end and in addition to other activities, IEC publishes International Standards, Technical Specifications, Technical Reports, Publicly Available Specifications (PAS) and Guides (hereafter referred to as "IEC Publication(s)"). Their preparation is entrusted to technical committees; any IEC National Committee interested in the subject dealt with may participate in this preparatory work. International, governmental and non-governmental organizations liaising with the IEC also participate in this preparation. IEC collaborates closely with the International Organization for Standardization (ISO) in accordance with conditions determined by agreement between the two organizations.
2) The formal decisions or agreements of IEC on technical matters express, as nearly as possible, an international consensus of opinion on the relevant subjects since each technical committee has representation from all interested IEC National Committees.
3) IEC Publications have the form of recommendations for international use and are accepted by IEC National Committees in that sense. While all reasonable efforts are made to ensure that the technical content of IEC Publications is accurate, IEC cannot be held responsible for the way in which they are used or for any misinterpretation by any end user.
4) In order to promote international uniformity, IEC National Committees undertake to apply IEC Publications transparently to the maximum extent possible in their national and regional publications. Any divergence between any IEC Publication and the corresponding national or regional publication shall be clearly indicated in the latter.
5) IEC itself does not provide any attestation of conformity. Independent certification bodies provide conformity assessment services and, in some areas, access to IEC marks of conformity. IEC is not responsible for any services carried out by independent certification bodies.
6) All users should ensure that they have the latest edition of this publication.
7) No liability shall attach to IEC or its directors, employees, servants or agents including individual experts and members of its technical committees and IEC National Committees for any personal injury, property damage or other damage of any nature whatsoever, whether direct or indirect, or for costs (including legal fees) and expenses arising out of the publication, use of, or reliance upon, this IEC Publication or any other IEC Publications.
8) Attention is drawn to the Normative references cited in this publication. Use of the referenced publications is indispensable for the correct application of this publication.

The main task of IEC technical committees is to prepare International Standards. However, a technical committee may propose the publication of a Technical Report when it has collected data of a different kind from that which is normally published as an International Standard, for example "state of the art".

IEC TR 63141, which is a Technical Report, has been prepared by IEC technical committee 104: Environmental conditions, classification and methods of test.

The text of this Technical Report is based on the following documents:

Draft TR	Report on voting
104/834/DTR	104/853A/RVDTR

Full information on the voting for the approval of this Technical Report can be found in the report on voting indicated in the above table.

This document has been drafted in accordance with the ISO/IEC Directives, Part 2.

The committee has decided that the contents of this document will remain unchanged until the stability date indicated on the IEC website under "http://webstore.iec.ch" in the data related to the specific document. At this date, the document will be

- reconfirmed,
- withdrawn,
- replaced by a revised edition, or
- amended.

IMPORTANT – The 'colour inside' logo on the cover page of this publication indicates that it contains colours which are considered to be useful for the correct understanding of its contents. Users should therefore print this document using a colour printer.

INTRODUCTION

Highly accelerated stress test (HAST), is a high temperature (100 °C or more), high humidity steady test of unsaturated pressurized steam of 85 % RH, and is the original test method that was developed for the evaluation of corrosion of packaged semiconductor wiring. This test method, often referred to as HAST, is applied to primarily non-hermetically sealed small electronic components, and has been standardized as a standard test method for evaluating, in an accelerated manner, the resistance to the deteriorative effect of high temperature and high humidity (IEC 60068-2-66). The equipment used for this test method is a chamber, filled with unsaturated water vapour, called a HAST chamber.

However, in life evaluation test conditions, acceleration cannot be obtained without air from the environment being incorporated into the HAST chamber. This test method is refetred to as air-HAST.

Examples of the application of air-HAST are whiskers evaluation of lead-free solder, deterioration life evaluation of conductive paste, and deterioration life evaluation of solar cells and are given in this document in order to provide an understanding of air-HAST with the aim, in future, to standardize air-HAST.

The International Electrotechnical Commission (IEC) draws attention to the fact that it is claimed that compliance with this document may involve the use of a patent concerning whisker evaluation given in Clause5.

IEC takes no position concerning the evidence, validity and scope of this patent right.

The holder of this patent right has assured the IEC that he/she is willing to negotiate licences under reasonable and non-discriminatory terms and conditions with applicants throughout the world. In this respect, the statement of the holder of this patent right is registered with IEC. Information may be obtained from:

ESPEC CORP.
3-5-6,Tenjinbashi,Kita-ku
Osaka,530-8550
Japan

Attention is drawn to the possibility that some of the elements of this document may be the subject of patent rights other than those identified above. IEC shall not be held responsible for identifying any or all such patent rights.

ISO (www.iso.org/patents) and IEC (http://patents.iec.ch) maintain on-line data bases of patents relevant to their standards. Users are encouraged to consult the data bases for the most up to date information concerning patents.

DAMP HEAT, STEADY STATE (UNSATURATED PRESSURIZED VAPOUR WITH AIR)

1 Scope

This document describes a new test method to control the volume of air injected into a conventional HAST chamber filled with water vapour. This document provides an overview of the conventional HAST chamber, an overview of the air-HAST equipment where air is incorporated into the HAST chamber, an example of an air-HAST test apparatus, and application examples of air-HAST.

2 Normative references

There are no normative references in this document.

3 Terms and definitions

For the purposes of this document, the following terms and definitions apply.

ISO and IEC maintain terminological databases for use in standardization at the following addresses:

- IEC Electropedia: available at http://www.electropedia.org/
- ISO Online browsing platform: available at http://www.iso.org/obp

3.1
galvanic corrosion
corrosion damage induced when two dissimilar materials are coupled in a corrosive electrolyte

3.2
Kirkendall effect
motion of the boundary layer between two metals that occurs as a consequence of the difference in diffusion rates of the metal atoms

3.3
whisker
metallic protrusion which grows up naturally during storage or in use

3.4
HAST
highly accelerated stress test
original test method developed to evaluate the corrosion of the semiconductor wiring at a high temperature of 100 °C or more

3.5
air-HAST
HAST test method with the addition of further air partial pressure in a HAST chamber

4 Overview of HAST and air-HAST

4.1 Overview of HAST chamber

4.1.1 Structure of HAST chamber

HAST is an evaluation test at a high-temperature and high-humidity unsaturated pressurized steam atmosphere environment of more than 100 °C. The test apparatus is roughly divided into a one-vessel type and a two-vessel type, as shown in Figure 1.

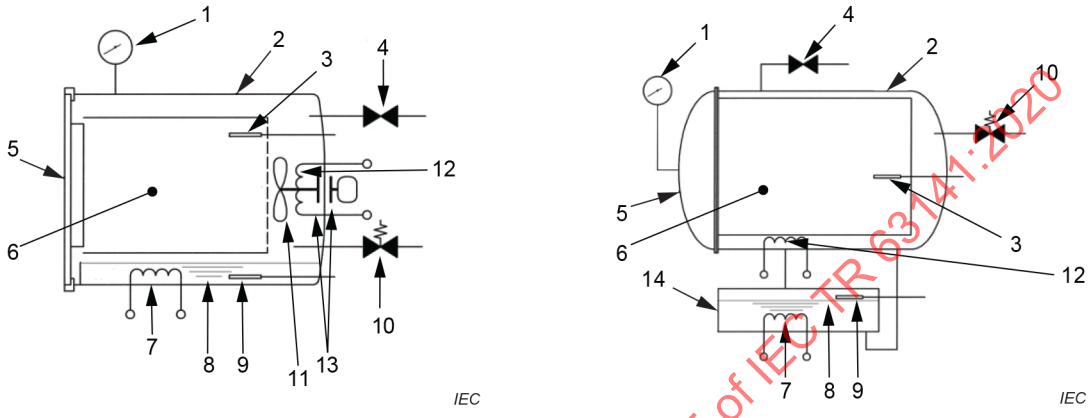

a) One-vessel type

b) Two-vessel type

Key

1 pressure gauge
2 pressure vessel
2 temperature sensor for moisture
4 safety valve
5 door
6 working space
7 heater for humidifying water
8 humidifying water
9 temperature sensor for humidifying water
10 air-exhaust valve
11 fan
12 heater for moisture fan for air
13 magnetic coupling
14 pressure vessel 2

Figure 1 – Two types of HAST equipment and their structures

The configuration of the one-vessel type and the configuration of the two-vessel type are explained as follows.

a) Configuration of the one-vessel type (See Figure 1 a))

This type of chamber is called a one-vessel type because it has only one pressure vessel. The inner cylinder provided inside the pressure vessel is divided into a steam generator for supplying humidifying water vapour and a working space to set the sample. A fan for generating a flow of steam from the steam generator to the working space is provided in the back of the inner cylinder. Heaters are arranged outside of this fan and in the steam generator. Steam flow rate of this system is suppressed to about the flow rate of natural convection.

b) Configuration of the two-vessel type (See Figure 1 b))

This type of chamber is called a two-vessel type because it is composed of two different pressure vessels: the test chamber which sets the sample and the steam generation chamber which supplies humidifying water vapour. Heaters are respectively located in the test chamber and the steam generation chamber. Water vapour is fed by boiling water vapour pressure to the test chamber from the steam generation chamber holding the humidifying water, the amount that was the condensed water goes back into the steam generation chamber. There is an inner cylinder in the test chamber, and a heater is provided on the outside of this inner cylinder. Heat from the heater is transmitted to the inner cylinder, keeping the temperature of the entire working space at a constant level. This system is also referred to as a natural convection because it does not require a fan for the circulation of water vapour.

4.1.2 Definition of humidity

HAST is carried out in a closed vessel which is isolated from the atmosphere of the atmospheric pressure (pressure vessel), under the assumption that air is absent from the filled water vapour atmosphere. Therefore during the start of HAST, steps to eliminate air (Figure 2 air vent process) are always taken. The humidifying water is heated and boiled by the heater, the exhaust valve is opened and the test vessel is filled with 100 % water vapour until all air is discharged. Then the exhaust valve is closed to perform heating until the test temperature in the vessel is reached again. The difference between the saturated test and unsaturated test in the working space in the chamber is then recorded. The state of the saturated test is shown in Figure 3. The state of the unsaturated test is shown in Figure 4. The air vent process is executed in both the saturated test and unsaturated test, the chamber needs to be filled with 100 % water vapour without air.

In saturation conditions, the working space is kept at a constant temperature by water vapour generated from the humidifying water because the heating source is only humidifying the water heater.

T_1: is the humidification water temperature;

T_2: is the test space temperature.

In this case the vessel temperature is $T_1 = T_2$.

In the case of the unsaturated test, a heater for heating the working space is installed in the chamber. In the apparatus, water vapour generated from the humidifying water enters the working space, it is re-heated by the heater to a higher temperature than the water vapour in the surroundings. When the temperature in the vessel is controlled to $T_1 < T_2$, the working space is an unsaturated vapour atmosphere. At this stage, the relative humidity (RH) of the working space is determined by the following equation:

$$H = P_1 / P_2 \times 100$$

where

H: is the relative humidity, RH (%);

P_1: is the saturated water vapour pressure in the humidification water temperature T_1 (MPa);

P_2: is the saturated water vapour pressure in the test space temperature T_2 (MPa).

At this stage the vessel pressure, P_1, is the test pressure because it is determined by the temperature of the humidification water (T_1).

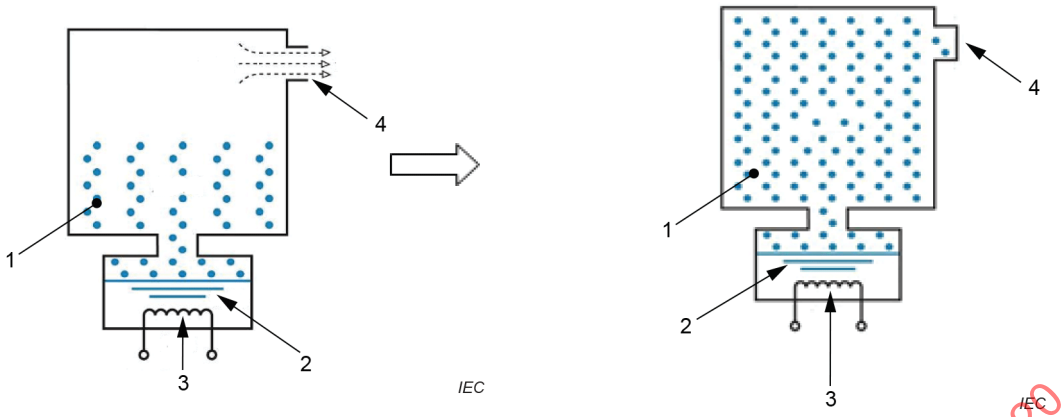

a) Air-exhaust valve open

b) Air-exhaust valve close

Key

1 water vapour
2 humidifying water
3 heater
4 air-exhaust valve

Figure 2 – Image of air vent process

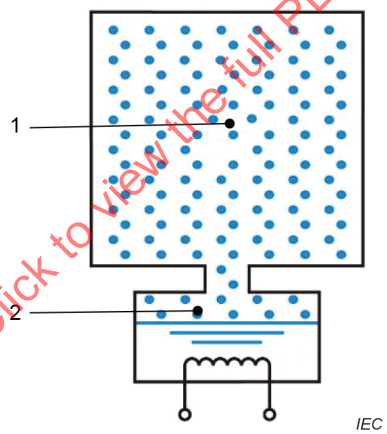

Key

1 working space
2 humidifying water

Figure 3 – Saturated test

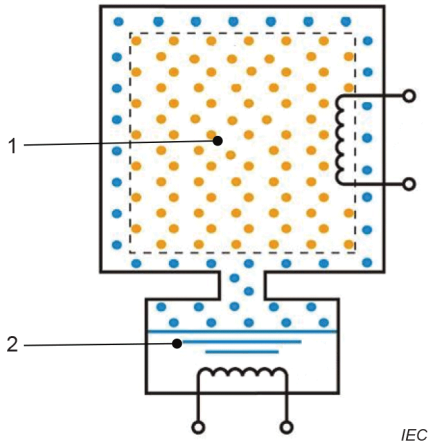

Key

1 working space

2 humidifying water

Figure 4 – Unsaturated test

4.2 Structure of air-HAST equipment

4.2.1 General

In the case of air-HAST, it is necessary to leave the air into a traditional HAST chamber. Considering the possibility that a residual air volume greatly affects test results, it becomes necessary to accurately control the amount of air. Using a conventional HAST chamber, to ensure the air-HAST environment contains air, the following two methods are used:

a) keeping a certain amount of air during start-up, and

b) injecting a predetermined amount of air after discharging air to the outside of the chamber.

Technically, either method is possible. Method a) can be realized simply by omitting the vent process, but it is difficult to control the amount of air to be discharged when adjusting the air volume. Method b) injects air after discharging air, so that the entire process becomes complicated but the control of the amount of air is easy. A dual-vessel type air-HAST chamber is shown in Figure 5. This equipment, which is a wet bulb installed and provided with a pan and wick temperature sensor in the working space of a conventional two-vessel type chamber, has become a mechanism for controlling the humidification water heater (steam generator) at the specified temperature. This air-HAST system is easily obtained from a dual-vessel type HAST equipment and has the advantage of facilitating experimentation. The method consists in injecting a predetermined amount of air from the air pressure port after the system has reached a steady state and all air in the chamber has been evacuated. The air remaining in the chamber is controlled by a pressure controller, so the constant partial pressure can be held.

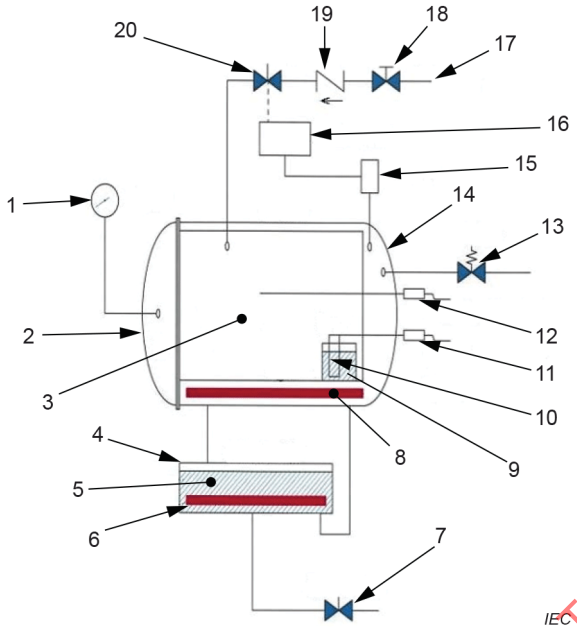

Key

1	pressure gauge	2	door	3	working space
4	pressure vessel 2	5	humidifying water	6	heater for humidifying water
7	solenoid valve for drain	8	heater for water vapour	9	wet bulb pan
10	cloth wick	11	sensor for humidifying water	12	sensor for water vapour
13	safety valve	14	pressure vessel 1	15	pressure sensor
16	pressure regulator	17	inlet	18	flow controller
19	check valve	20	solenoid valve		

Figure 5 – Structure of two-vessel type air-HAST chamber

A one-vessel air-HAST chamber (Figure 6) is used for whiskers, electrically-conducting adhesives and photovoltaic modules reliability tests. A one-vessel air-HAST chamber is of a less complex constitution providing reproducible and compatible test results. At first, the specimen is set in the vessel at room temperature, the door is closed, the test is started to create heat and humidity. This way there is no pressure damage by a sudden change in pressure and no condensation on the specimen. In addition, a forced steam of water-vapour is normally generated by means of a fan installed in the chamber to create air velocity and accurately detect humidity by a dry and wet bulb.

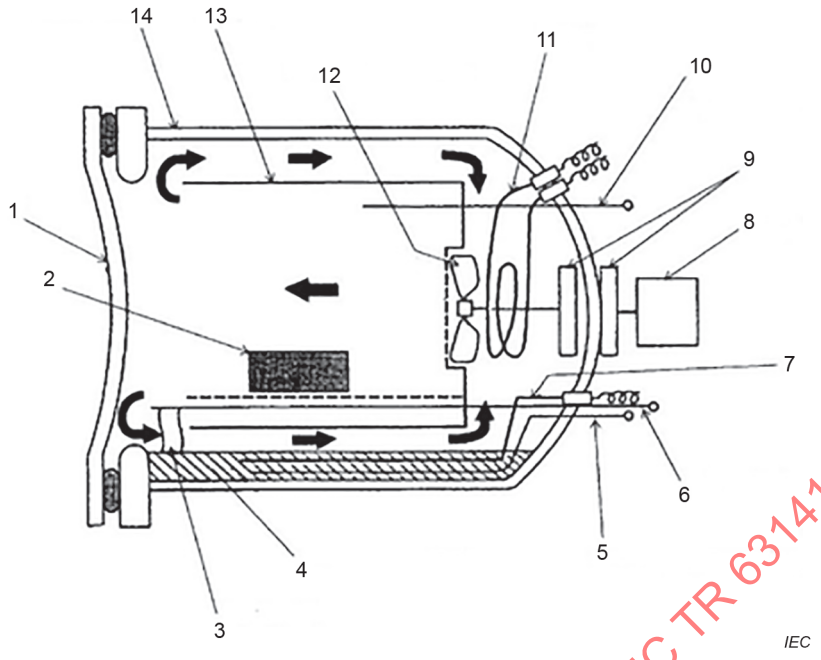

Key

1 door	2 specimen	3 cloth wick
4 humidifying water	5 humidifying water temperature sensor	6 wet bulb temperature sensor
7 humidifying heater	8 air circulating fan motor	9 magnetic coupling
10 chamber temperature sensor	11 heater	12 air circulating fan
13 inner cylinder	14 pressure vessel	

Figure 6 – Structure of one-vessel type air-HAST chamber

4.2.2 Air concentration and relative humidity

Initially the intention was to determine the exact concentration of oxygen using an oxygen concentration meter. However, since the inside of the HAST equipment reaches a high pressure up to 1 atm or more, a commercial oxygen concentration meter operating in such an environment was not available.

Therefore, the amount of air is calculated based on the gauge pressure. Moreover, since it is difficult to measure the correct relative humidity directly in an air-HAST chamber, relative humidity is controlled by the temperature in the same way as for a conventional HAST chamber.

5 Evaluation of tin whisker growth from lead-free plating and solder-joints

5.1 Whisker of lead-free solder (comb-type substrate)

5.1.1 General

Lead-free manufacturing of electronic products has now reached its implementation stage and around 2 000, the focus was moved to finding a solution to suppress tin whisker growth. Related studies are still on-going.

Clause 5 describes the results of the studies, and how the whiskers generated from the corrosion of solder joints or plated surface are accelerated by high-temperature and high-humidity conditions; conventional HAST with temperatures exceeding 100 °C does not give the expected further acceleration and good acceleration is achieved only with air-HAST with additional air partial pressure [1] to [11][1].

5.1.2 Summary of evaluation results of solder-joint whisker growth [3] [4]

5.1.2.1 Test method

Figure 7 shows examples of the test vehicles with comb pattern conductors. The conductor width and the conductor spacing in Figure 7 a) are both 0,318 mm. In Figure 7 b) the conductor width and the conductor spacing are both 0,165 mm. These vehicles are submitted to preconditioning as described in Figure 8 with Sn-3Ag-0,5Cu solder. The coated flux on the comb pattern substrate consists of a mass fraction of 75 % of IPA (isopropyl alcohol) and a mass fraction of 25 % of WW (water white) rosin with the addition of a varied amount of diethylamine hydrobromide as an activator. Environmental test conditions are given in Table 1 and Figure 9 shows pressure, temperature and humidity profiles for both the HAST (Figure 9 a)) and air-HAST test chambers (Figure 9 b)).

a) Large pitch (comb pattern 1) **b) Small pitch (comb pattern 2)**

Figure 7 – Example of test vehicle with comb pattern

Table 1 – Test conditions

Test type	Test condition
High temperature/high humidity	55 °C/85 % RH
	75 °C/85 % RH
	85 °C/85 % RH
HAST	110 °C/85 % RH (Air partial pressure 0 kPa)
Air-HAST	110 °C/85 % RH (Air partial pressure 130 kPa)[a]
[a] Theoretical value.	

[1] Numbers in square brackets refer to the bibliography.

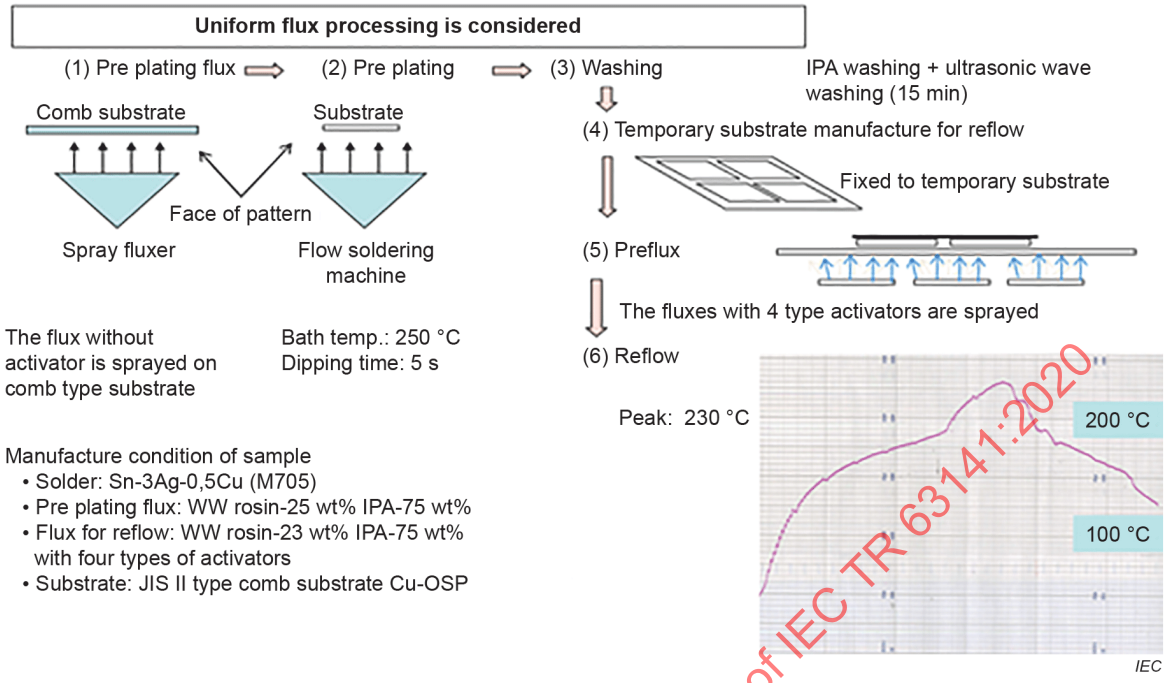

Figure 8 – Process flow for sample build

HAST (wet and dry bulb controlled) conditions are:

Total pressure: 0,121 8 MPa abs, 0,03 MPa G.

Air-HAST conditions are:

Total pressure: 0,251 8 MPa abs, 0,15 MPa G.

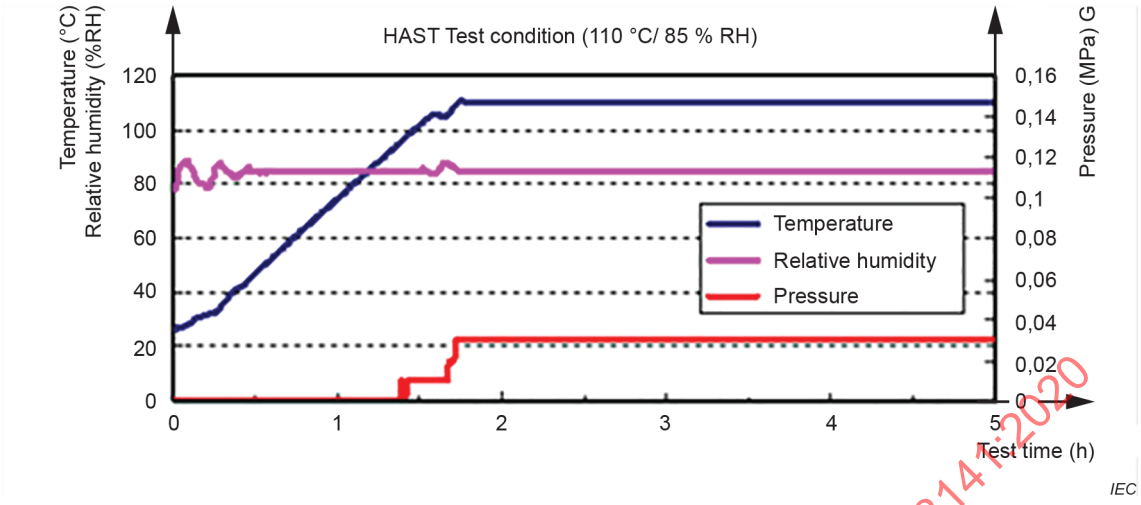

a) HAST temperature/relative humidity profiles

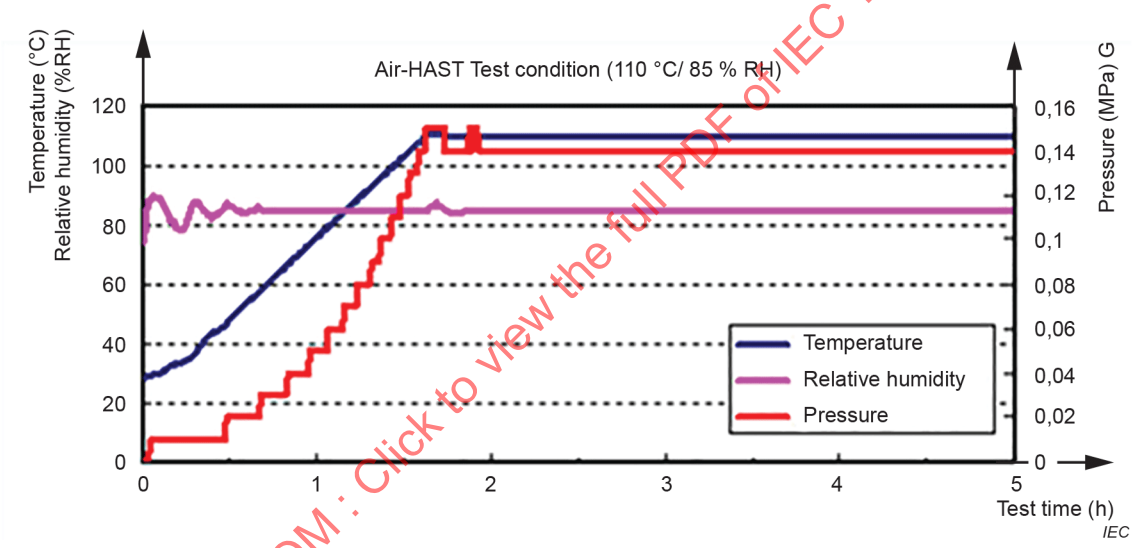

b) Air-HAST temperature/relative humidity profiles

NOTE 1 Both absolute pressure (abs) and gauge pressure (G) are shown.

NOTE 2 Total pressure of air-HAST is set at 0,251 8 MPa, as the sum of partial pressure of air (0,130 MPa) and water vapour (0,121 8 MPa).

NOTE 3 Gauge pressure = Absolute pressure – 0,101 3 MPa (atmospheric pressure).

Figure 9 – Temperature/relative humidity profiles of HAST and air-HAST

5.1.2.2 Test results

The results of the temperature-humidity tests are shown in Table 2. Growth of whiskers was observed in early stages with a bromine-based flux. The acceleration by temperature was also observed from the test with varied temperatures. Air-HAST equipment with a single test chamber as shown in Figure 6 was used for an acceleration property study. Although conventional HAST in the region of 110 °C/85 % RH for test vehicles with a bromine-based flux exhibited no whisker growth as shown in Table 3, air-HAST – with added air partial pressure – exhibited whisker growth from an early stage as shown in Table 4 [3] [4]. Examples of such whiskers are shown in Figure 10.

Table 2 – Influence of fluxes and circumstances to whisker growth

Activator	Diethyl amine HBr salt				
Content wt %	0,1	2	2	2	4
Temperature (°C)	85	85	70	55	85
Humidity (% RH)	85	85	85	85	85
500 h	None	40 µm	-	-	45 µm
1 000 h	None	67 µm	None	None	44 µm
1 500 h	None	91 µm	None	None	63 µm
2 000 h	None	83 µm	16 µm	None	87 µm
3 000 h	-	102 µm	35 µm	None	-
4 000 h	-	125 µm	86 µm	None	-
5 000 h	-	153 µm	64 µm	None	-
7 000 h	-	160 µm	110 µm	20 µm	-
10 000 h	-	208 µm	112 µm	17 µm	-

Table 3 – Whisker generation in HAST

No.	Flux	Solder composition	Pattern	HAST (110 °C /85 % RH)			
				200 h	300 h	400 h	600 h
1	Flux none	Sn-3Ag-0,5Cu	Large	None	None	None	None
2			Small	None	None	None	None
3	Bromine system flux		Large	None	None	None	None
4			Small	None	None	None	None

Table 4 – Whisker generation in air-HAST

No.	Flux	Solder composition	Pattern	Air-HAST (110 °C 85 % RH)					
				50 h	100 h	150 h	200 h	300 h	400 h
1	Flux None	Sn-3Ag-0,5Cu	Large (A)	None	None	None	None	None	None
2			Small (B)	None	None	None	None	None	None
3	Bromine system flux		Large (A)	None	None	38 µm	15 µm	28 µm	46 µm
4			Small (B)	None	30 µm	37µm	36 µm	53 µm	90 µm

No.	Test Vehicle	Air-HAST (110 °C / 85 % RH)					
		50 h	100 h	150 h	200 h	300 h	400 h
3	Large (A)	None	None	38 µm	15 µm	28 µm	46 µm
4	Small (B)	None	**30 µm**	**37 µm**	36 µm	53 µm	90 µm

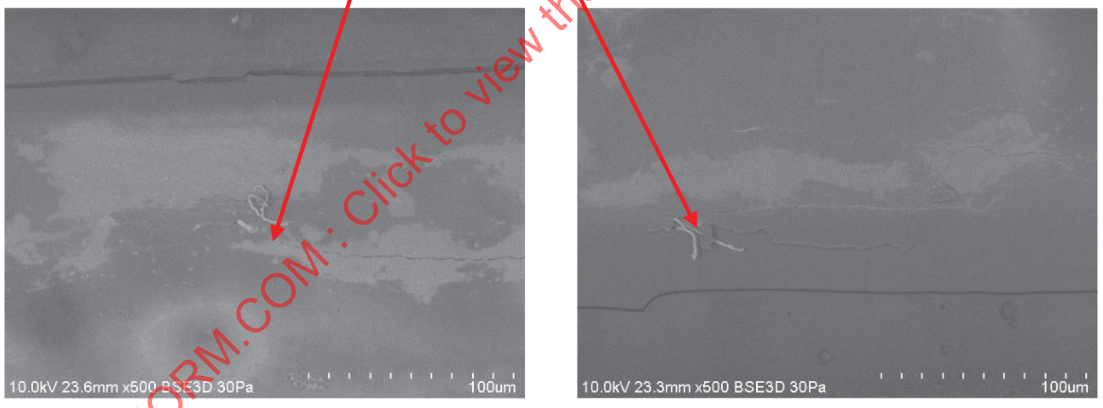

IEC

Figure 10 – Whisker generation situation in air-HAST

Ohno et al reported that the whisker growth is accelerated by localized solder corrosion enhanced by the residue of bromine-based activator [5].

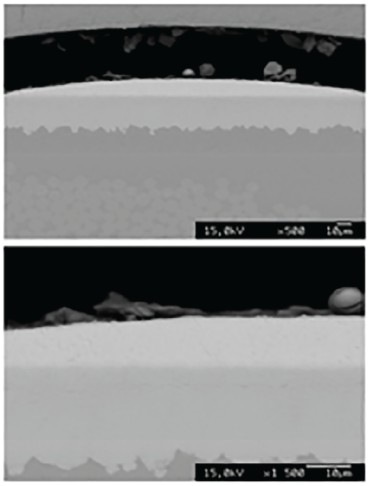

IEC

a) Reflected electron image

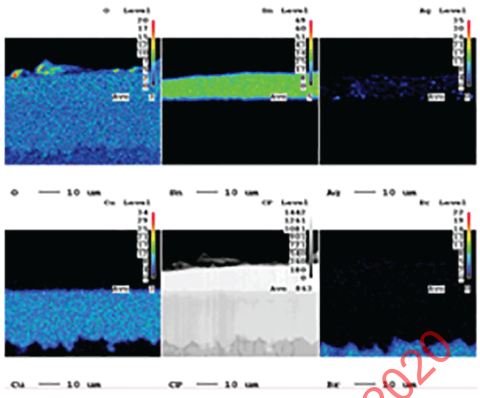

15,0 kV × 1 500

IEC

b) Elementary analysis

Test conditions:

110 °C/85 % RH 200 h

Solder: Sn-3Ag-0,5Cu

Flux: Bromine system flux

Figure 11 – Mapping of the cross-section at the solder fillet in HAST

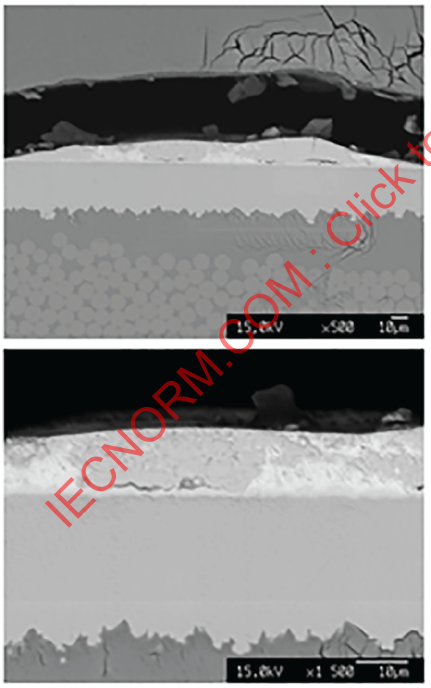

IEC

a) Reflected electron image

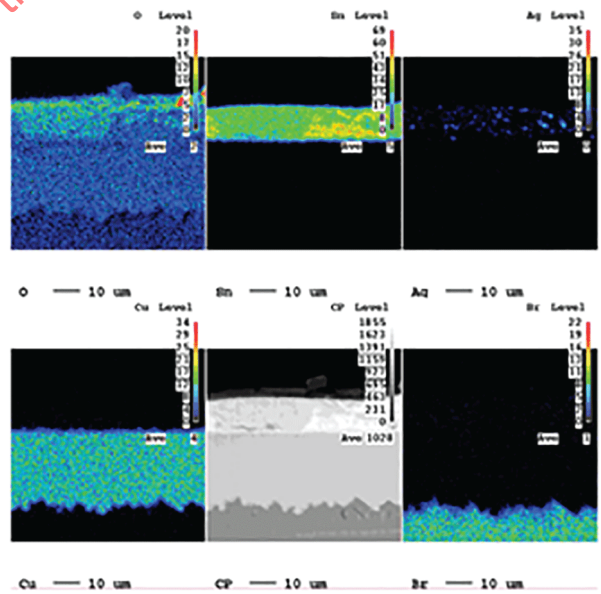

15,0 kV × 1 500

IEC

b) Elementary analysis

Test conditions:

110 °C/85 % RH 200 h

Solder: Sn-3Ag-0,5Cu

Flux: Bromine system flux

Figure 12 – Mapping of the cross-section at the solder fillet in air-HAST

Cross-section observation of samples from these HAST and air-HAST tests are shown in Figure 11 and Figure 12. Figure 11 shows no corrosion in the solder layer, even after 200 h of HAST exposure with no apparent whisker growth, while in Figure 12, showing the result of the air-HAST test, oxygen penetration into the solder layer was observed. These results correspond to whisker growth [3].

5.1.2.3 Effect of oxygen on solder whisker generation [3]

The previous results indicate that, in addition to humidity, the presence of oxygen is necessary for the generation of whisker. Electrochemical reactions of tin, with the effect of oxygen included, were derived as follows. Tin transfers to oxide by way of hydroxide as these formulae indicate.

$$Sn \rightleftharpoons Sn^{2+} + 2e^{-} \quad (1)$$

$$O_2 + 2H_2O + 4e^{-} \rightleftharpoons 4OH^{-} \quad (2)$$

$$Sn^{2+} + 2OH^{-} \rightleftharpoons Sn(OH)_2 \quad (3)$$

$$Sn(OH)_2 + 2OH^{-} \rightleftharpoons SnO_2 + 2H_2O + 2e^{-} \quad (4)$$

Tests to evaluate electrochemical migration (ECM) was also conducted, and ECM was observed without any air partial pressure, thus indicating its mechanism is different from that of whisker generation [7].

5.1.2.4 Acceleration property from varied humidity test [3]

5.1.2.4.1 General

Whisker generation evaluation was conducted on test boards with comb-pattern conductors, with Sn-3Ag-0,5Cu solder and a mass fraction of 2 % flux with a bromine-based activator. The environmental test conditions were based on standard conditions of 85 °C/85 % RH. Temperatures ranging from 55 °C to 110 °C (typical air-HAST conditions) with a constant humidity of 85 % RH were used. Humidity ranging from 65 % RH to 85 % RH with a constant temperature of 85 °C was applied. The time needed for whisker growth of approximately 20 µm was defined as time-to-whisker L (hours) and used throughout the study.

5.1.2.4.2 Time-to-whisker versus temperature with constant humidity

The results of the test with a constant relative humidity of 85 % RH and varied temperatures are shown in Figure 13. The figure shows good linearity on an Arrhenius plot (relationship between reciprocal of absolute temperature and time-to-whisker on a logarithmic scale). Air-HAST was employed at a temperature of 110 °C. Good linearity was obtained over a wide range of test temperatures. Activation energy E_a was calculated from the slope of this plot as 0,84 eV.

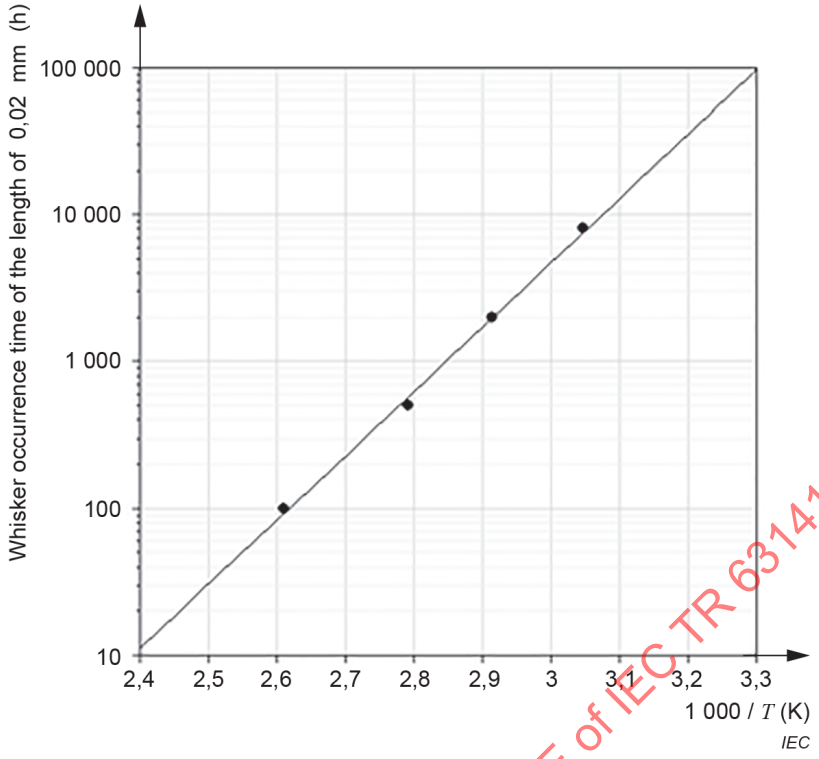

Figure 13 – Arrhenius plot of the bromine-based flux

5.1.2.5 Discussion on lifetime characteristic formulae

Various formulae were proposed for lifetime characteristics. The Arrhenius plot, among others, is widely known for temperature changes using the reciprocal of absolute temperature, and exhibited good linearity as shown in Figure 13.

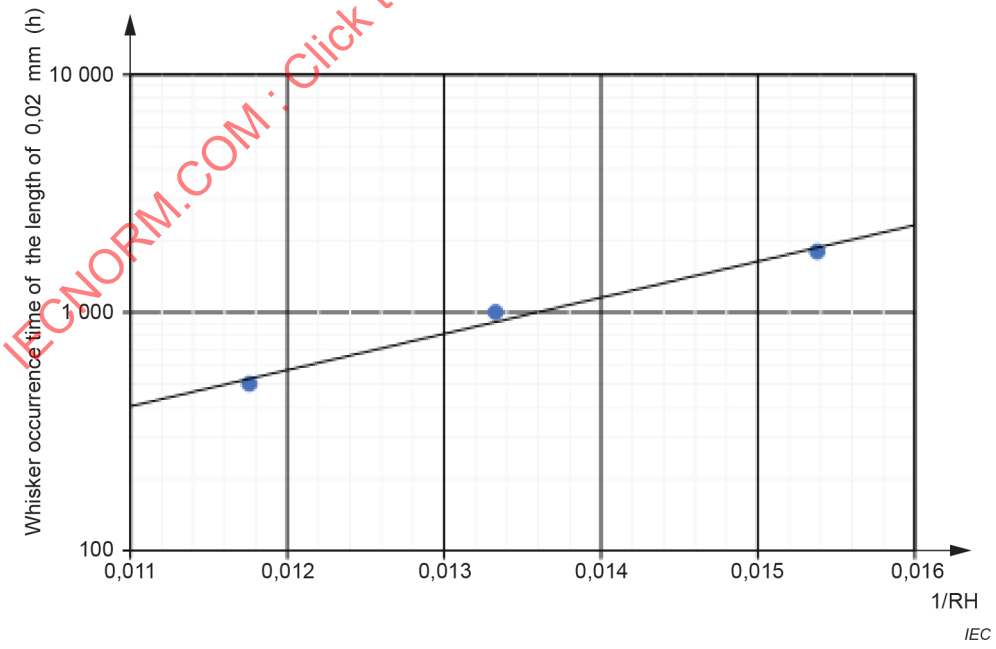

Conditions:

Solder: Sn-3Ag-0,5Cu

Temperature: 85 °C

Figure 14 – Reciprocal of relative humidity of whisker generation on solder

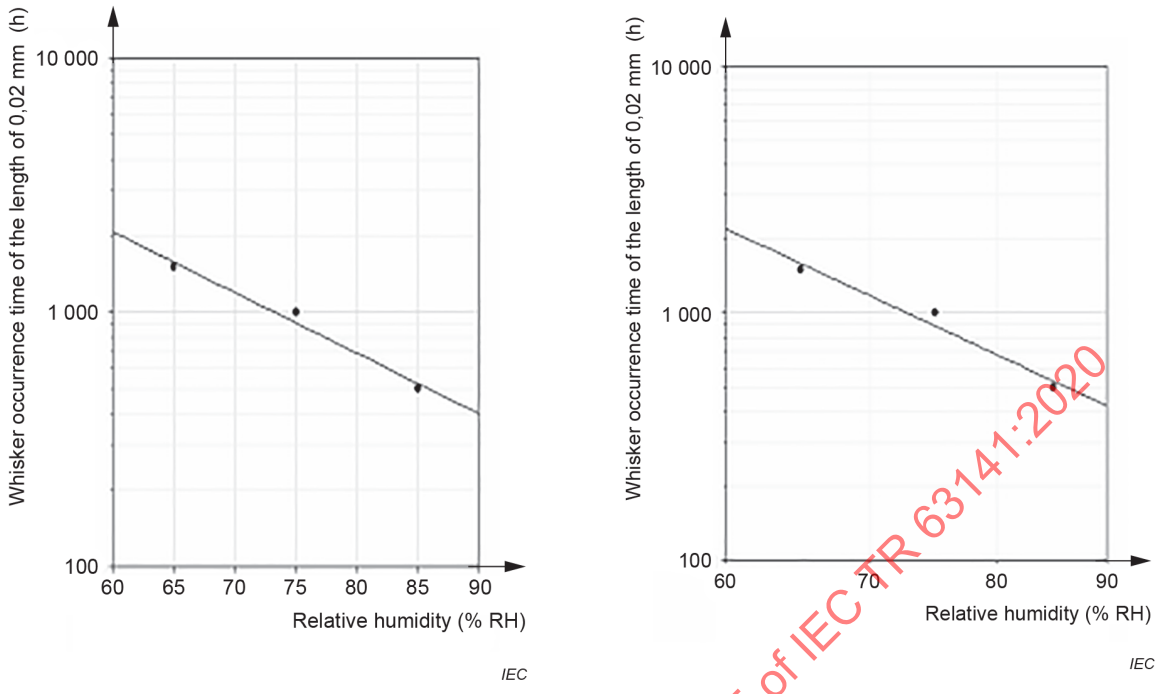

a) Linear plot of relative humidity **b) Logarithmic plot of relative humidity**

Conditions:

Solder: Sn-3Ag-0,5Cu

Temperature: 85 °C

Figure 15 – Humidity properties of whisker generation on solder (pt.2)

When the relative humidity is changed at a constant temperature of 85 °C, the ordinate represents the logarithm of the time until whisker generation, and the abscissa represents the reciprocal of the relative humidity as shown in Figure 14.

The vertical axis in Figure 15 a) and Figure 15 b) is the time required for the whisker length to reach 0,002 mm. Figure 15 a) is a linear scale of relative humidity on the horizontal axis, and Figure 15 b) is a display showing relative humidity logarithmically. The straight line approximation gives a good agreement and is expressed as Equation (5).

An Arrhenius plot with temperature, related to the effects of humidity change, has not been established so far. Therefore for the presentation of relative humidity on the abscissa, there are four proposals:

a) as reciprocal,

b) on a linear scale,

c) on a logarithmic scale [8],

d) humidity characteristics utilizing the relationship of vapour pressure of water and absolute temperature.

Results of the solder-joint whisker growth test are used for curve fitting, using proposals a) to c) above. Relative humidity in a) and b) are indicated as exponential for the purpose of combination of temperature characteristics to an Arrhenius plot. The results are shown below as Equations (5) to (7).

$$L_1 = A_1 \exp(E_a/kT + B/\ \%\ \mathrm{RH}) \quad (5)$$

$$L_2 = A_2 \exp(E_a/kT - C \cdot \%\ \mathrm{RH}) \quad (6)$$

$$L_3 = A_3 \cdot (\%\ \mathrm{RH})^{-m} \exp(E_a/kT) \quad (7)$$

Here, E_a (activation energy) is 0,84 eV as shown in 5.1.2.4.2 and k is a Boltzmann constant. B is obtained from the linear approximation of Figure 14 which is a logarithm plot of the time-to-whisker L with respect to the reciprocal of relative humidity. Similarly, C is obtained from Figure 15 a) which is the plot with the relative humidity as the horizontal axis, and m is obtained from the plot with the logarithm of relative humidity as the horizontal axis. The obtained coefficients B, C and m are shown in Table 5. In the same table, results of other studies on various degradation phenomena are cited from literature. The results of these three equations for whisker growth from solder-joint show no significant difference in R^2 (coefficient of determination, $0 \leqq R^2 \leqq 1$). Model (5) is slightly better. This model is the same as a model used for whiskers on plated tin (iNEMI) [1]. The values of the coefficients, however, are close to those for the increase in contact resistance of conductors or ECM [9] [11]. This was attributed to the difference in corrosion progress speed, since solder-joint and conductive adhesive had a far thicker layer of plating. Furthermore, the conductor resistance of conductive adhesive has approximately the same value as that of coefficient B, in relation to relative humidity, but has much smaller activation energy E_a, of approximately the same value as for whiskers from plated tin. These models can be used for the calculation of L for changes in temperature and humidity, thus making it possible to calculate the acceleration factor of acceleration test conditions of temperature and humidity, compared to the actual usage conditions [12].

5.1.3 Conclusion

The studies conducted on the effect of different types of flux on, and acceleration methods for, the growth of whiskers generated on tin-free solder-joint of Sn-3Ag-0,5Cu solder have led to the following conclusions.

Table 5 – Comparison of coefficients for Equations (5), (6) and (7)

		E_a (eV)	B (% RH)	C (% RH)$^{-1}$	m	Reference
(1)	Tin whisker on solder-joint	0,84	$2{,}98 \times 10^2$	$5{,}5 \times 10^{-2}$	4,06	IEC TR 63141
	R^2	0,996	0,94	0,97	0,96	
(2)	Tin whisker on plating					iNEMI[1]
	3 μm thick	0,31	-	$3{,}1 \times 10^{-2}$	-	(R^2 = 0,94)
	10 μm thick	0,28	-	$1{,}7 \times 10^{-2}$	-	(R^2 = 0,72)
(3)	Conductive adhesive					
	Contact resistance	0,78	$6{,}05 \times 10^2$	-		ESPEC [9]
		0,8	$3{,}00 \times 10^2$	$5{,}7 \times 10^{-2}$ [a]	4,0[a]	SCAS [10]
	Conductor resistance	0,38	$2{,}35 \times 10^2$	-	-	RCJ [11]
(4)	ECM	0,75	$2{,}95 \times 10^2$	$5{,}2 \times 10^{-2}$ [a]	4.0[1)]	T. L.Welsher [12]

NOTE R^2 is the coefficient of determination.

[a] Estimated from figures in literature.

1) Non-uniform oxidation corrosion develops on solder-joints, when they are kept in high-temperature and high-humidity conditions, and becomes a major cause of the generation of whiskers.

2) Flux with a bromine-based activator is a cause of solder corrosion. With other types of flux it takes 5 to 10 times longer to generate whiskers.

3) Using flux containing a bromine-based activator and Sn-3Ag-0,5Cu solder, good linearity was obtained on an Arrhenius plot within the temperature range of 55 °C to 110 °C (with constant humidity of 85 % RH). The calculated activation energy E_a was 0,84 eV. Air-HAST was used for the 110 °C test, since HAST was found to suppress the growth of whiskers and has no acceleration effect.

4) Good correlation and good fitting of models was obtained when the relative humidity was assigned to the abscissa axis, compared to assigning reciprocal or logarithm of relative humidity.

5) Activation energy E_a and coefficients of humidity response of whiskers from solder-joints were compared to other degradation phenomena. These values were found to be larger, compared to whisker growth from tin plating, and similar to contact resistance changes between conductive adhesive and tin plating, and ECM.

5.2 Lead-free whisker of plating (mounting substrate)

5.2.1 General

Creating lead-free electronic devices leads to risks of short circuit failures caused by whiskers formed from semiconductor lead frames. Since few studies exist on whisker formation in semiconductor packaging substrates, causes and mechanisms of the phenomenon have not been completely explained. This document analyses how different plating materials, substrates and environmental test conditions create different whisker formation conditions, and provides an experimental analysis of their formation causes [13] [16].

5.2.2 Test method

5.2.2.1 Sample evaluation

The samples used were QFP-mounted substrates. Table 6 lists their details and they are shown on Figure 16. Table 7 describes the lead frame composition. Two substrate types (Cu and Fe-Ni) and four plating types (Sn, Ni-Pd-Au [shortened here to 'Pd'], Sn-Cu and Sn-Bi) were used. Fe-Ni substrate samples with the Pd plating were not used.

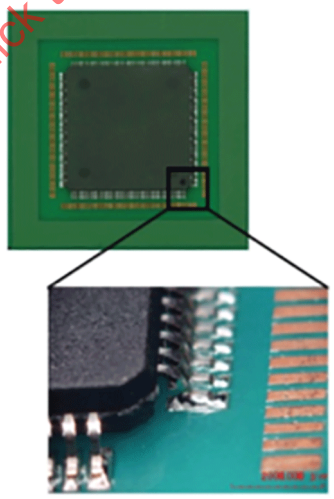

IEC

Figure 16 – Evaluated sample

Table 6 – Details of evaluated samples

Tested package	QFP (176 pins)
Board material	FR-4
Solder paste	Sn-3Ag-0,5Cu
Reflow peak temperature	240 °C
Sample quantity	2 of each (Cu substrate / Sn only × 4)

Table 7 – Lead frames composition

Substrate	Plating	Average plating thickness
Cu	Sn Sn-Cu Sn-Bi	10 µm
	Ni-Pd-Au	Ni 1,17 µm Pd 0,03 µm Au flash
Fe-Ni	Sn Sn-Cu Sn-Bi	10 µm

5.2.2.2 Test method

Environmental test conditions are given in Table 8. A temperature cycling test (with a 15-min holding time), high-temperature/high-humidity test and highly accelerated stress test (HAST) were performed. It was also investigated whether the presence of oxygen affected whisker formation by conducting an air-HAST test, with air remaining in the chamber. The samples were removed after arbitrary test times, and the leads were observed under optical and scanning electron microscopes. After observation, the same samples were put back into the test chamber.

Table 8 – Environmental test conditions

Test name	Conditions
Temperature cycling	-40 °C/85 °C 15 min each
High Temperature/High humidity	55 °C/85 % RH
High Temperature/High humidity	85 °C/85 % RH
HAST	110 °C/85 % RH (air pressure 0 kPa)
Air-HAST	110 °C/85 % RH (Air pressure 130 kPa theoretical value)

5.2.3 Test results

5.2.3.1 General

Figure 17 shows the whiskers' morphology.

Test conditions	Pd	Sn	Sn-Bi	Sn-Cu
Temperature cycling test (-40 °C/85 °C) 3 000 cyc	Partial observation and undetected	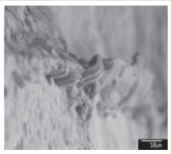 Nodule 20 µm	Partial observation and undetected	 Nodule 15 µm
High temperature/ high humidity test (55 °C/85 % RH) 3 000 h	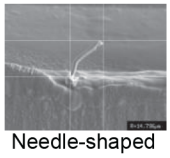 Needle-shaped 20 µm	Partial observation and undetected	--	-
High temperature/ high humidity test (85 °C/85 % RH) 1 000 h	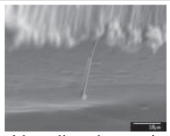 Needle-shaped 20 µm	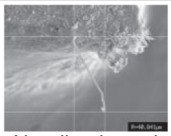 Needle-shaped 40 µm	-	-
HAST (110 °C/85 % RH) 200 h	Partial observation and undetected	Partial observation and undetected	-	-
Air-HAST (110 °C/85 % RH) Air pressure 130 kPa 200 h	Partial observation and undetected	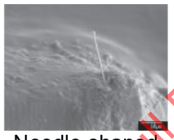 Needle-shaped 25 µm	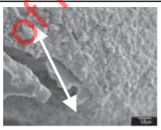 Needle-shaped 80 µm	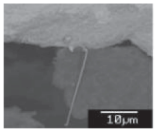 Needle-shaped 30 µm

IEC

Figure 17 – Whisker formation (Substrate: Cu)

5.2.3.2 Differences due to test conditions

As shown in Figure 17, the temperature cycling tests formed needle-shaped and nodular whiskers. The whiskers formed under high-temperature/high-humidity tests and air-HAST tests were mostly needle-shaped, but some were nodular.

Whiskers did not form after 3 000 h of high-temperature/high-humidity test at 55 °C/85 % RH, but a small number of whiskers formed after 200 h of air-HAST testing. No whisker formation after 200 h of HAST testing was found. The whisker formation in the air-HAST test environment may have been aided by the presence of oxygen.

5.2.4 Observations

The formation of whiskers may be attributable to the following causes [17]:

a) formation of intermetallic compounds;

b) formation of oxides due to corrosion; and

c) repeated compression and expansion.

Whisker formation may be caused by complex interactions among causes a) to c). In this experiment, these complex factors were accelerated by the test environment, and each factor was emphasized by the environmental test conditions. On Cu substrates in a high-temperature environment for example, growth occurs at the solder/intermetallic compound interface. As shown in the cross-section observation of Figure 18, it was confirmed that intermetallic compounds grow relative to the initial phase during temperature cycling and at high temperature during high-temperature/high-humidity testing. It was conjectured that the main components of the generated intermetallic compounds are Cu_3Sn and Cu_6Sn_5.

Volumetric expansion is thought to generate a compressive stress since Cu_6Sn_5 has a greater volume than Cu.

Test conditions	Lead extremity	Lead shoulder portion
Start	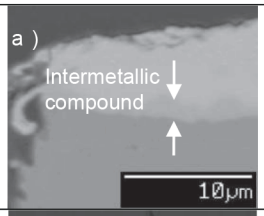	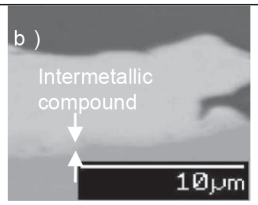
Temperature cycling test (-40 °C/85 °C) 3 000 cyc	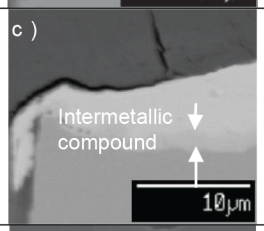	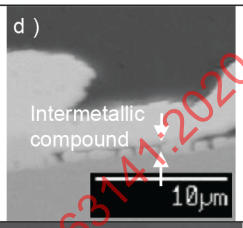
High temperature/ high humidity test (55 °C/85 % RH) 3 000 h	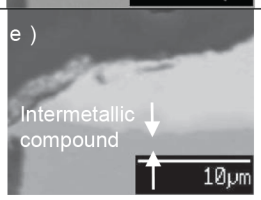	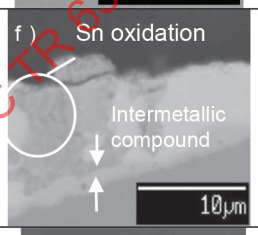
High temperature/ high humidity test (85 °C/85 % RH) 1 000 h	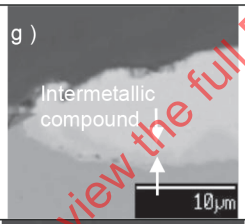	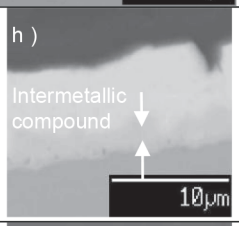
HAST (110 °C/85 % RH) Air pressure 0 kPa 200 h	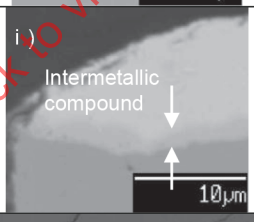	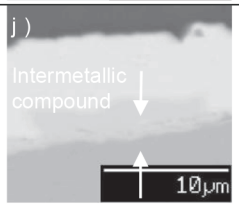
Air-HAST (110 °C/85 % RH) Air pressure 130 kPa 200 h	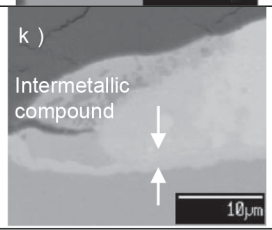	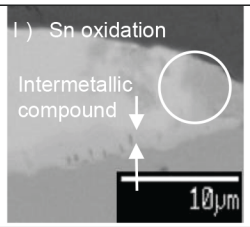

IEC

Figure 18 – Cross-section inspection results with electron-imaging (Substrate: Cu)

Surface oxidation of Sn due to corrosion was also confirmed. Almost no initial-phase surface oxidation was observed. After air-HAST and high-temperature/high-humidity testing, surface observations showed blackening of lead ends and shoulder parts. Cross-sectional observations showed that plating and solder were not uniform on each lead, and some samples showed significant oxidation in the vicinity of exposed substrate as shown in (f) and (l) of Figure 18.

The oxygen present during air-HAST testing favoured oxide generation from corrosion more than in samples subjected to high-temperature/high-humidity testing at 55 °C/85 % RH.

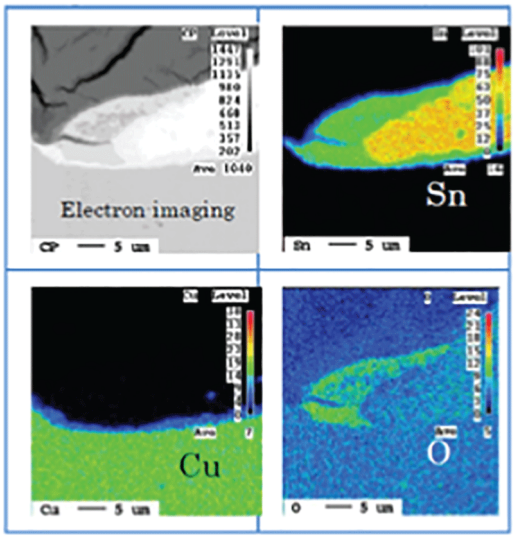

IEC

Figure 19 – Elements analysis

Moreover, the high-temperature environment of air-HAST testing also encouraged the generation and growth of intermetallic compounds, potentially enabling short-duration whisker evaluations. An example is illustrated in Figure 19. The lead extremities of the air-HAST samples showed significant generation of Cu and Sn alloy layers and Sn oxides between the plating and substrate. Since SnO_2 has a greater volume than Sn, cases in which Sn in the solder oxidized into SnO_2 are thought to be the result of compressive stress generated by volumetric expansion [13].

5.2.5 Conclusion

Whisker formation was found in the soldering of the tested QFP lead plating regardless of plating type and even if the plating did not contain Sn.

Various environmental conditions are linked to whisker formation. Whisker formation is greatly affected by the generation of intermetallic compounds at high temperatures, by the generation of oxides from corrosion at high humidity, and by repeated compression and expansion during temperature cycles.

Air-HAST testing (at 110 °C/85 % RH) has the potential to accelerate whisker formation since it has a greater effect on the generation of intermetallic compounds and the generation of oxides from corrosion than high-temperature/high-humidity testing (at 55 °C/85 % RH).

Substrate differences during a temperature cycling test affect whisker formation. Cu substrates may form whiskers due to the generation of intermetallic compounds, and Fe-Ni substrates may form whiskers due to repeated compression and expansion.

In a future report, the mechanisms will be thoroughly explained by continuing environmental testing and carrying out further analysis of the whiskers' formation sites.

6 Applied case of JISSO using electrically-conductive adhesive and acceleration test under humidity environments for joining parts

NOTE "JISSO" is the integration of materials, electronic components, modularization, and assembly to realize some function (or specification). As there is no equivalent English expression, the Japanese term "JISSO" is used worldwide.

6.1 General

The purpose of this study is to demonstrate that it is possible to estimate the lifetime of conductive adhesive in humidity testing. In order to reduce the causes of failure modes, types of components are restricted to a chip resistor.

Because the evaluation of conductive adhesive of the product level by high reliability in typical humidity testing is time-consuming, a way to accelerate evaluation further and reduce the time was investigated.

HAST is usually used in conditions of more than 100 °C of acceleration area, but it does not follow the Arrhenius law to evaluation for joining because there is a small quantity of oxygen.

It was verified that air-HAST, when there is oxygen, follows the Arrhenius law as well as the humidity test at temperatures lower than 100 °C and can be applied up to 120 °C [11] to [18].

6.2 Experiment method

6.2.1 Testing material

Conductive adhesives used in the test are a silver epoxy standard conductive adhesive (components of which are disclosed) as shown in Table 9 and a commercially available electrically conductive adhesive.

Table 9 – Electrically-conductive adhesives

Type of electrically-conductive adhesives	Symbol
In the epoxy resin of a resin combination system (the normal composition to make the phenomenon easy to understand for evaluation). It includes a metallic filler such as silver of a mass fraction of 70 % to 80 %, and additionally it improves the viscosity of material such as paste which contains a reaction diluent and curing agent.	XA-5554A
A resin combination system (marketed product)	A

The mounted component was the chip resistor (1608R) which was one of the general surface mount components from the point of easy analysis. An example of mounted component is shown in Figure 20.

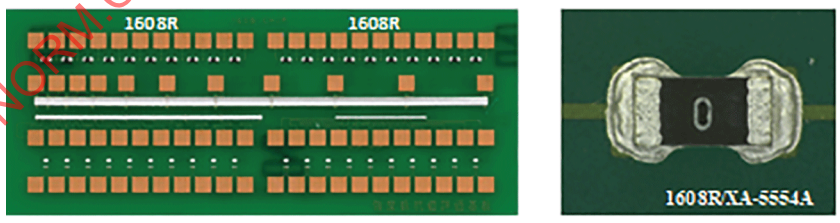

IEC

Figure 20 – Substrate for conductive resistance measurement and example of component mounting

6.2.2 Test conditions

Test conditions are shown in Table 10. Air-HAST conditions (120 °C/85 % RH + air) were introduced, in addition to the usual humidity conditions because it took a long time to evaluate.

Table 10 – Testing material

Component/Figure	Type	Electrode composition		
		Base-material	Undercoat	Outermost layer
Chip resistor	1608R	Ag	Ni	Sn

Degradation of the inside of the components and the only conductive adhesive deterioration is small. Resistance change caused by the reaction of the resin component of the conductive adhesive and the electrode plating components of the bonding interface due to the influence of moisture was focused. The conductive resistance was measured in continuity as shown in Figure 21 in each test environmental test condition.

The one-vessel type Air-HAST test equipment as shown in Figure 6 was used.

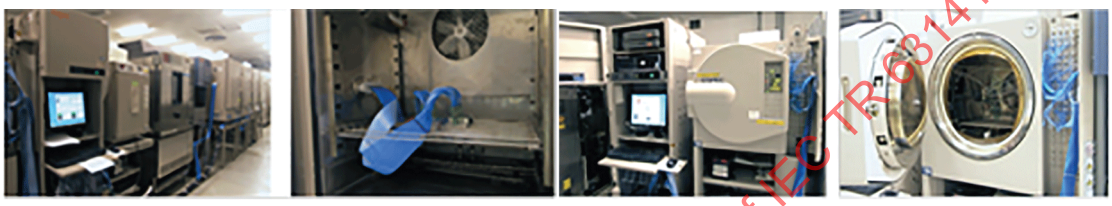

IEC

Air-HAST is shown on the far right photograph.

Figure 21 – Humidity test conductive resistance monitor test status

6.2.3 Measurement and evaluation method

The procedure for the evaluation method is as follows:

a) conductive resistance continuous monitor in each environment state;
b) data analysis of conductive resistance value;
c) Weibull statistical analysis of conductive resistance value;
d) life estimation;
e) cross-section analysis (EDX,SEM);
f) consideration of deterioration factor.

6.3 Test results

6.3.1 Experimental result

After confirming that the conductive resistance value continuously rose as shown in Figure 22, time when conductive resistance value was doubled compared to the initial value was picked out as a failure time.

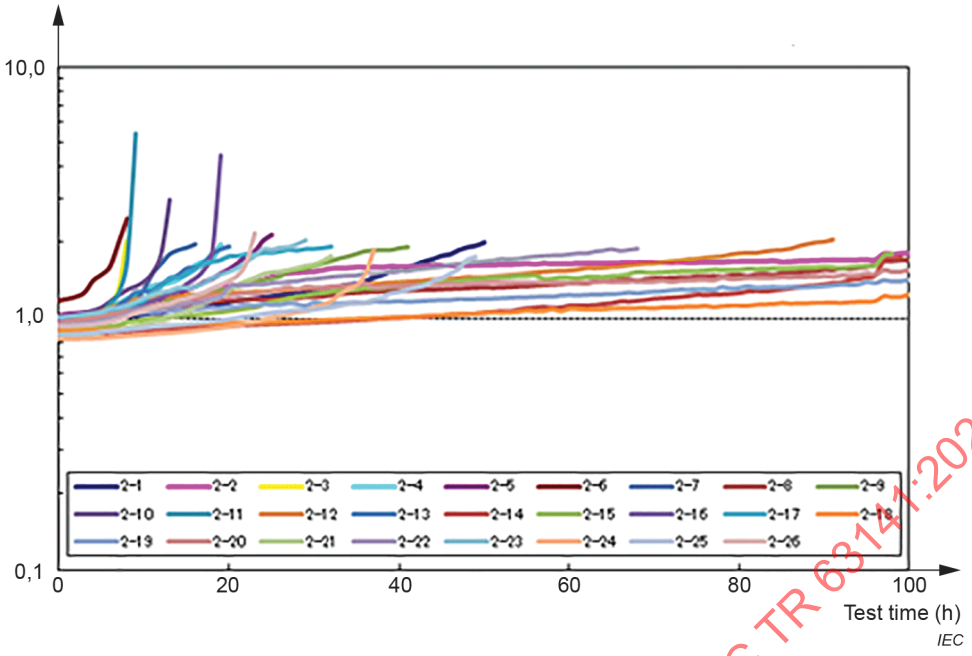

Figure 22 – Example of the conductive resistance value change

Weibull statistical analysis was performed based on getting the failure time except the abnormal value and the outlier and the Weibull parameter B_{10} life was calculated.

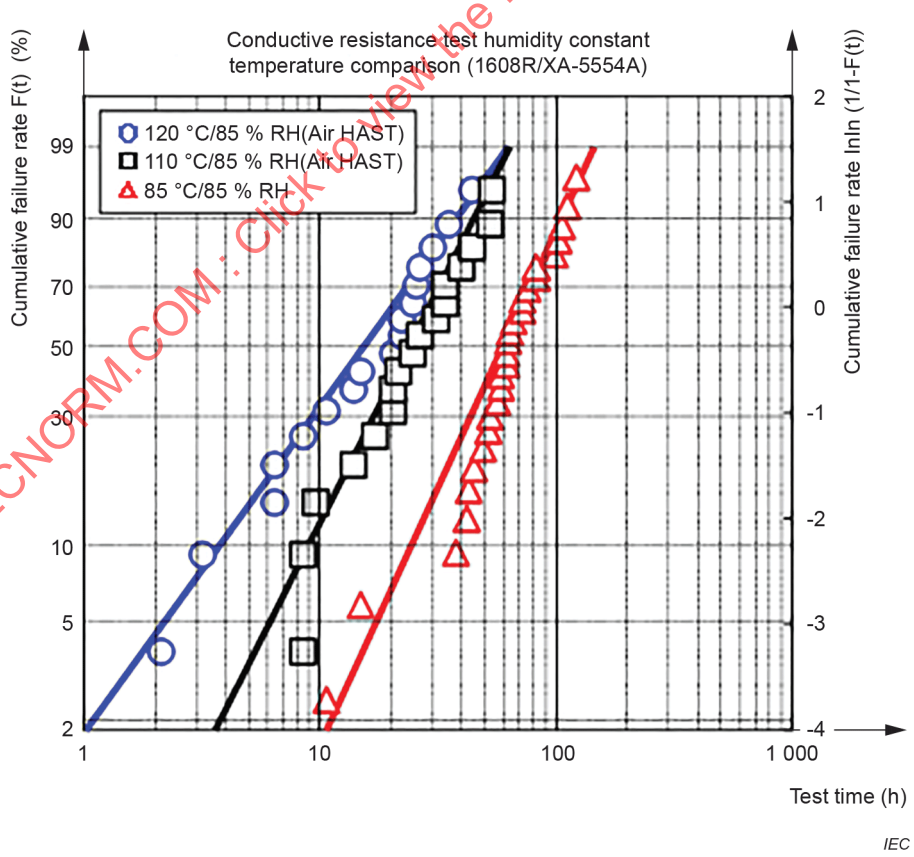

Figure 23 – Weibull plot of temperature acceleration (under fixed humidity conditions)

B_{10} life, which was obtained from the graph in Figure 23 with different temperature and humidity constants, was plotted according to the Arrhenius model shown in Equation (8).

$$L = A \cdot \exp\left(\frac{E_a}{kT}\right) \Rightarrow \ln L = \frac{E_a}{kT} + \ln A \quad (8)$$

where

E_a is the activation energy;

T is the absolute temperature;

k is the Boltzmann constant.

As a result, Figure 24 was obtained and the activation energy E_a was calculated as 0,61 eV.

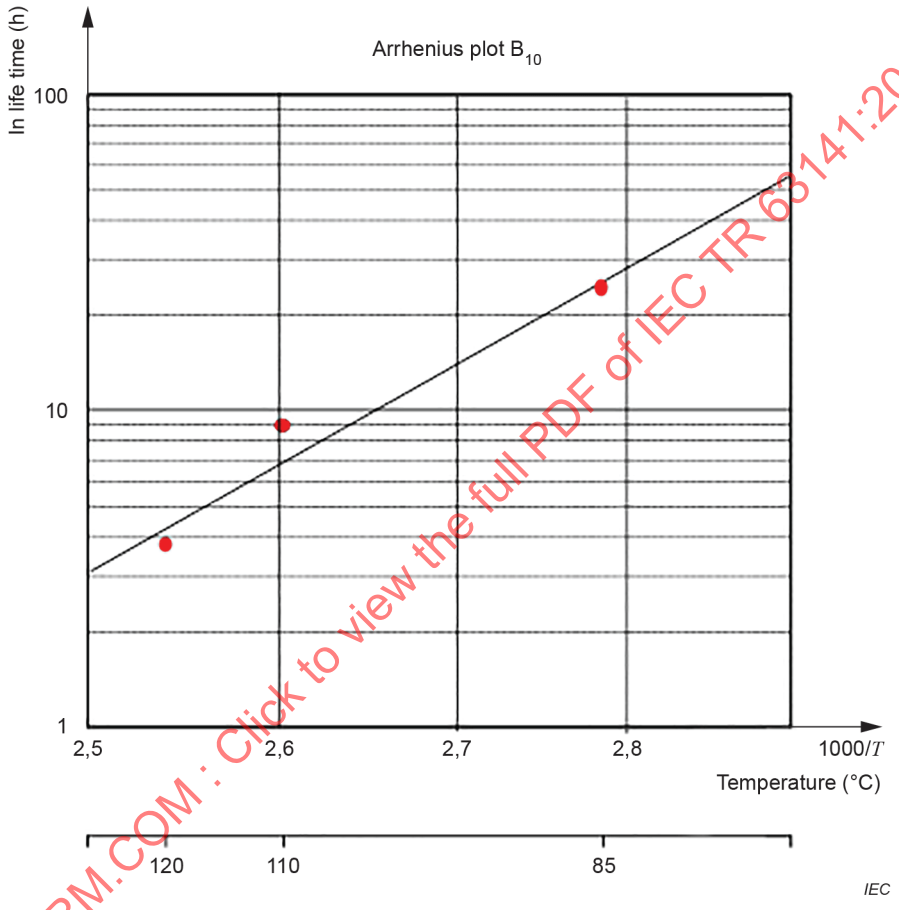

Figure 24 – Arrhenius plot (fixed humidity)

As shown in Figure 24, experiments were made with air-HAST with air and with conventional HAST with water-vapour atmosphere, at a temperature range above 100 °C.

In this way, in an acceleration test with corrosion, air-HAST has been first substantiated to be able to obtain good linearity by Arrhenius plot in temperatures above 100 °C:

$$L \propto \exp\left[\frac{E_a}{kT}\right] \cdot \exp\left[\frac{B}{RH}\right] \quad (9)$$

where

E_a: is the activation energy;

T: is the absolute temperature;

k: is the Boltzmann constant;

B: is a constant;

RH: is the relative humidity.

$$\ln L = \left[\frac{E_a}{kT} + \frac{B}{RH} \right] + b \tag{10}$$

Formula (9) has been known as a relational expression of the lifetime when changing the relative humidity at a temperature of 85 °C. The plot, which is based on Formula (9) as a representative value of B_{10} from the Weibull plot in Figure 25, is shown in Figure 26.

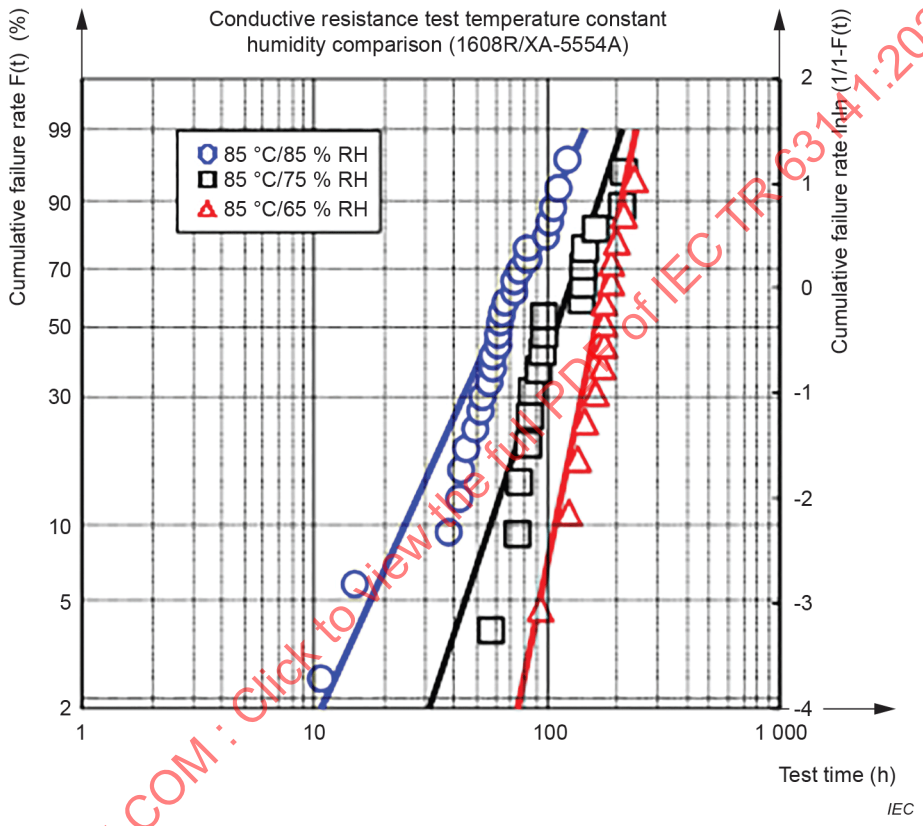

Figure 25 – Weibull plot of humidity acceleration (under fixed temperature conditions)

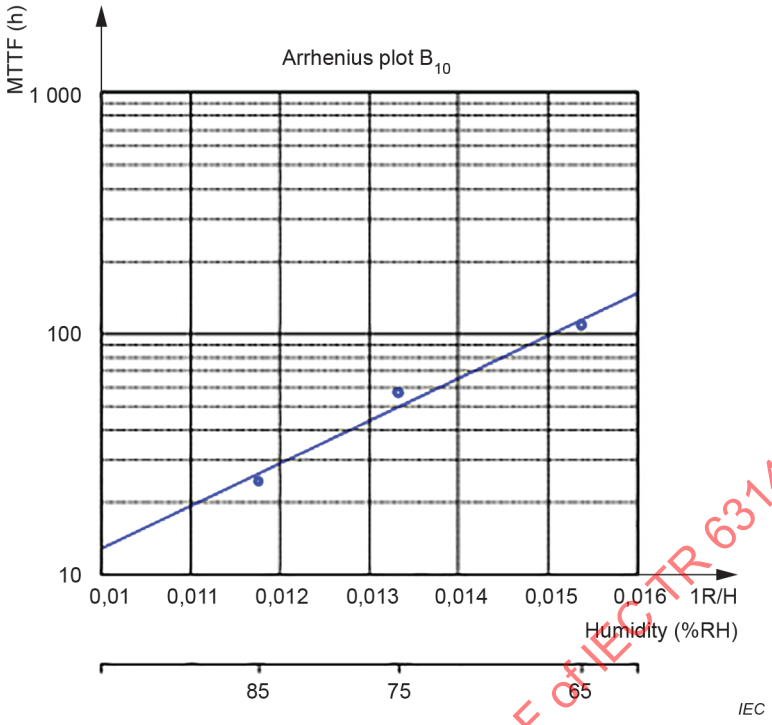

Figure 26 – Arrhenius plot (fixed temperature)

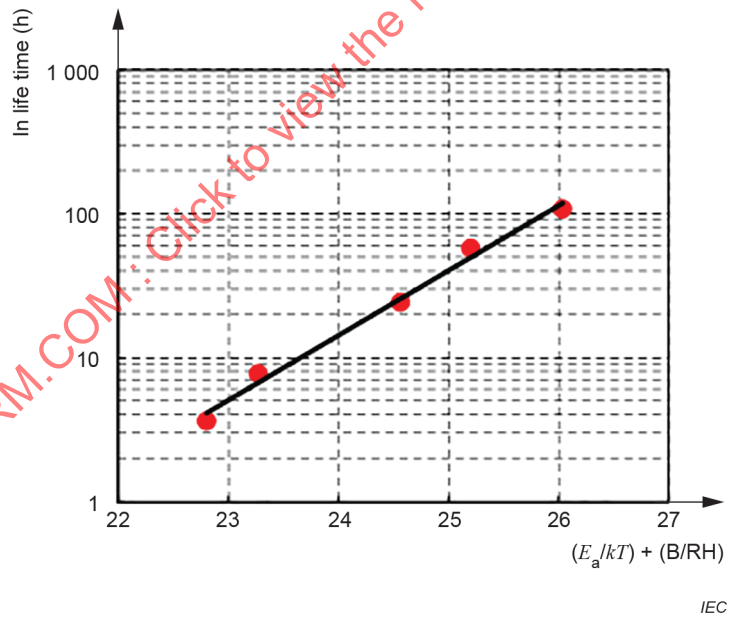

Figure 27 – Eyring plot of all conditions

The value 407(RH)$^{-1}$ as the constant B of Formula (9) from a slope is shown on Figure 26.

Additionally, Formula (10) (Eyring model) that combines temperature and humidity is known. In accordance with this formula, Figure 27 can be obtained by plotting the data taken in [E_a/kT + B/RH] on the horizontal axis. A good linearity was also obtained in this case.

Since the result of each test condition was on the straight line in the Eyring plot as shown in Figure 27, air-HAST conditions were confirmed to exhibit the same acceleration as in normal humidity test conditions of less than 100 °C.

Then, the activation energy (E_a) is the oxidation energy of the interface of the electrically-conductive adhesive and electrode, its acceleration factor is the relation to the concentration of water and temperature in the neighborhood of the interface.

6.3.2 Test result (1608R/paste A)

Among the electrically-conductive adhesive under test as shown in Table 11, the test result of paste A was described.

Table 11 – Test conditions

Humidification method	Test environmental condition	Test time/method of measurement
Usual temperature/ temperature conditions	(85 °C/85 % RH), (85 °C/75 % RH), (85 °C/65 % RH)	2 000 h Conductive resistance measurement in continuity
Air HAST condition	(110 °C/85 % RH), (120 °C/85 % RH)	100 h to 300 h Conductive resistance measurement in continuity

Since paste A is a good commercial product resistant to temperature and humidity, no change was observed under the normal temperature and humidity conditions.

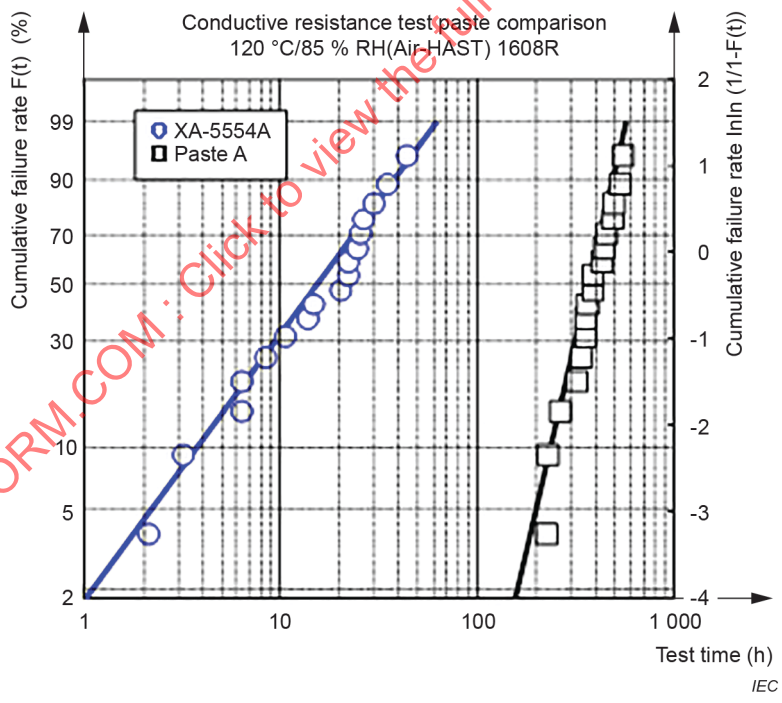

Figure 28 – Comparison of paste (120 °C/85 % RH Air-HAST)

As shown in Figure 28, the only change was confirmed in most severe conditions (120 °C/85 % RH air-HAST). From the B_{10} life of the Weibull statistical analysis result, the lifetime of paste A is 63 times longer than that of the XA-5554A. Therefore, it was confirmed that paste A offers better resistance properties to temperature and humidity.

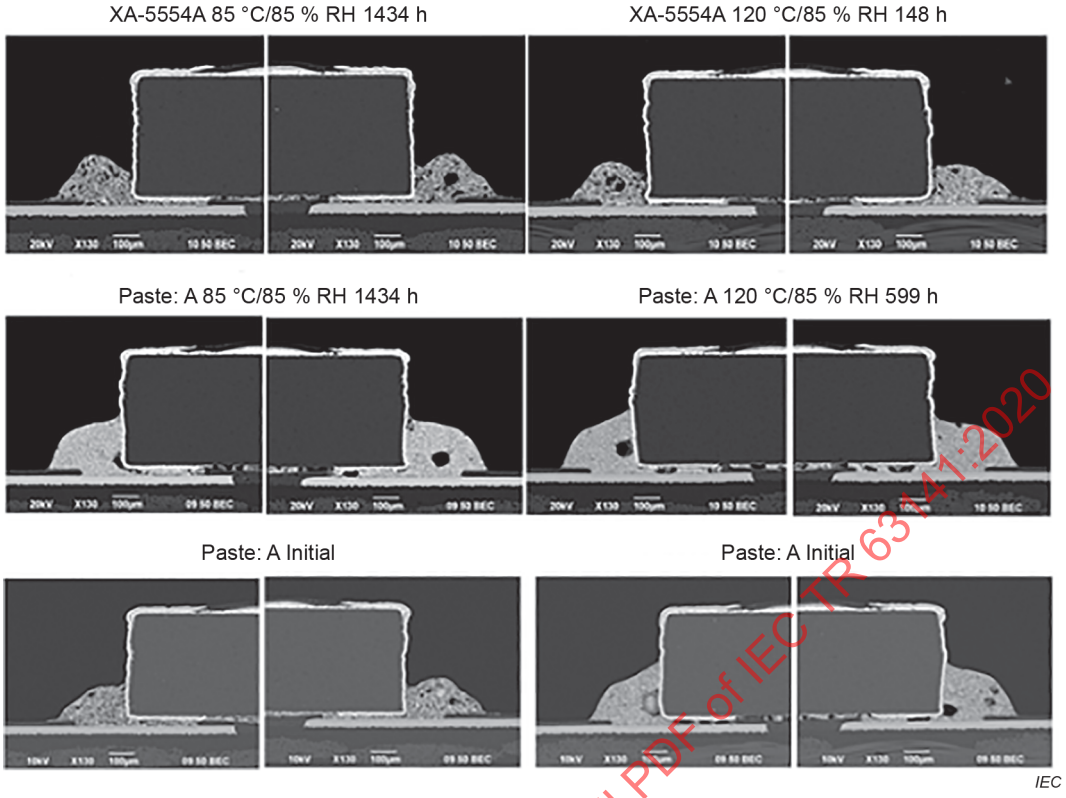

Figure 29 – Cross-section analysis of 1608R after a humidity test (SEM image)

The cross-sectional SEM photographs of 1608R before and after the test are shown in Figure 29. In the case of XA-5554A, some voids were confirmed in joint interface after testing, but were not confirmed in the initial state. In the case of paste A, there were more voids during curing than in the initial state, but the test results are considered to have little influence.

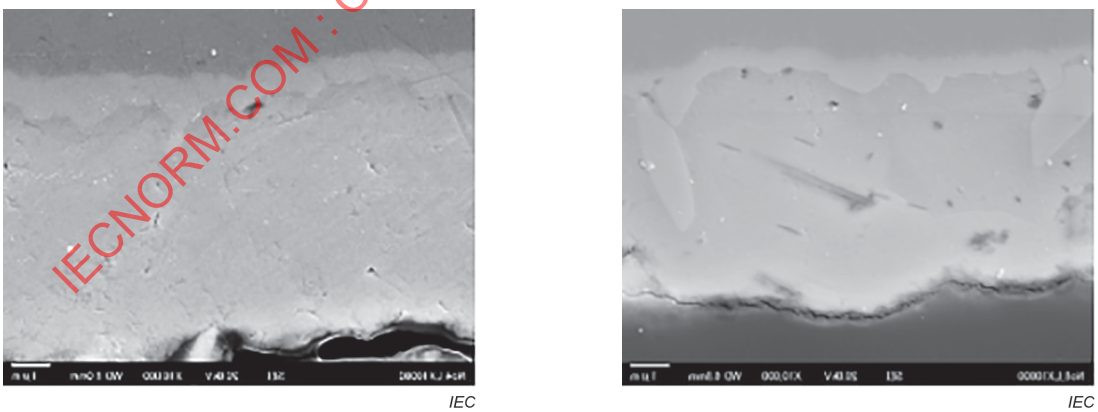

a) 85 ℃/85 % RH⑧ 1 434 h × 10 000 b) 120 ℃/85 % RH④ 781 h × 10 000

Figure 30 – Magnified image of cross-section analysis of 1608R after a humidity test (SEM image)

As shown in Figure 30, using more magnification, cracks between the copper foil and resin interface were not observed in a short duration test, but voids were observed in the copper interface in a long duration test.

Moreover, because the same configuration is shown in either test condition from component analysis results by EDX as shown in Figure 31, it is believed that the degradation mode is the same. Because a degradation mode is identical, change in resistance plotted by each test condition in Figure 27 shows that the application of the Eyring model is reasonable.

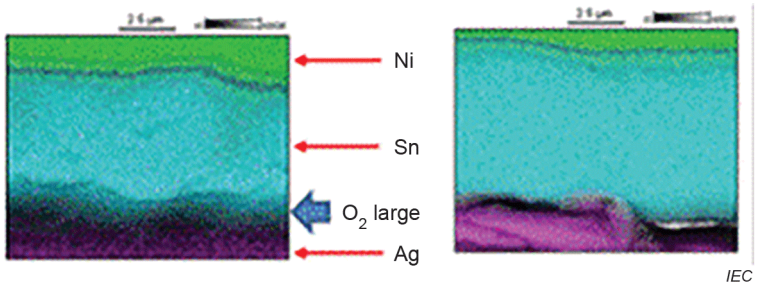

Figure 31 – Cross-section analysis of 1608R after a humidity test (SEM image) and examples of componential analysis by EDX

Interfacial cracks are observed in the final extraction. In the short duration test cracks are not observed in the interface between a copper foil and resin. Because it is a high acceleration test, during the resistance value change, the voids are observed in the Sn layer as shown in Figure 31. Therefore, it is considered that voids are related to galvanic corrosion and the Kirkendall effect.

6.4 Points of attention

Air-HAST equipment is a remodeled conventional HAST equipment in order to conduct air-HAST testing. It was performed in the surface finishing field as the way to make acceleration metallic oxidation corrosion originally.

Air-HAST environment is a high pressure environment compared to the conventional HAST environment, in terms of the amount of poured air. Therefore, for such a component bonding, it is necessary to sufficiently consider not to corrode until the unintended state. It is considered that a test duration of more than 100 h is inappropriate.

6.5 Summary

The International Standard on electrically-conductive adhesive, ISO 16525 (all parts), was published in 2014. A humidity test in the environmental testing method is specified in Part 7. Although test conditions are specified as the quality criteria, it is important to evaluate short duration tests for new product development.

The result of an air-HAST is confirmed to show the same degradation as in the humidity test with temperatures less than 100 °C compared to the conventional HAST.

The Arrhenius model and Eyring model are applied for various conditions and the results of the various conditions are arranged in a straight line shape as shown in Figure 27. Therefore air-HAST can be used for the moisture resistance accelerated evaluation of the metal junction.

7 Applied air-HAST to c-Si PV modules evaluation tests

7.1 Background and objective

The situation surrounding photovoltaic power generation has been rapidly changing in Japan and overseas, marked by market growth and the rapid rise of Asian emerging countries as production bases. In these circumstances, the start of Japan's feed-in tariff scheme in July 2012 has seen a rush of so-called 'megasolar' construction projects around the country. But reducing the cost of solar generation still remains a pressing problem. Several issues should be tackled to lower costs, improving photovoltaic module efficiency and lowering production costs, along with improving reliability and increasing device life.

Despite these pressing needs, however, technology to evaluate the life of crystalline silicon photovoltaic modules ('photovoltaic modules') has not been developed yet, and there are demands for methods of evaluating long-term reliability. The environment testing used in IEC 61215-1 for crystalline silicon modules is design qualification and type approval, and is done mainly for the purpose of screening tests. Tests with extended test times are therefore carried out to ensure long-term reliability, leaving the issue of long test times.

The effect of temperature and humidity on the deterioration of photovoltaic modules were investigated, as part of a research topic examining the development of new accelerated test methods for shortening test times, etc. by means of accelerated testing and highly accelerated testing that combine major deterioration factors. This report presents an investigation of accelerated testing for extended high-temperature/humidity testing and high temperature/humidity testing [22].

7.2 Photovoltaic module structure and deterioration factors

Figure 32 shows the structure of a photovoltaic module. A photovoltaic cell is created to form electrodes on the surface where N-type and p-type semiconductors are joined. Under standard conditions of solar radiation intensity of 1 000 W/m^2, air mass coefficient of 1,5 and cell temperature of 25 °C, the DC power generation capacity of a single cell of about 10 cm × 10 cm in size is at 0,5 V and 3 A. So to obtain the power output required for various applications, it is necessary to increase the voltage by connecting multiple cells in series using wire called interconnectors.

The surface is covered with reinforced glass, and a back surface material (backsheet) is used, surrounded by filler material. A frame is added to complete the module. Table 12 shows examples of failure and deterioration factors for photovoltaic modules.

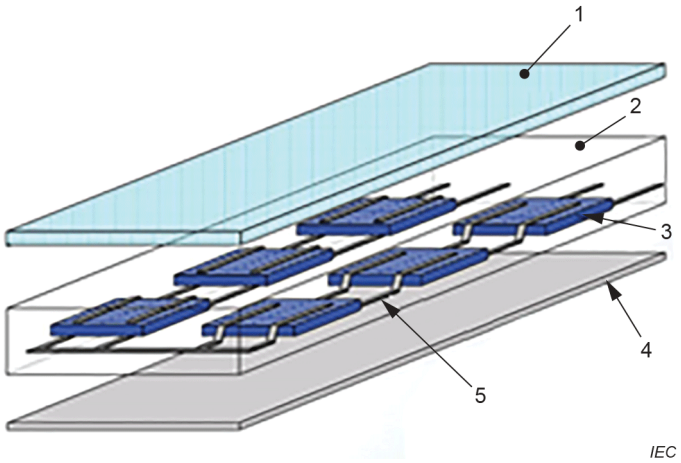

Key

1 glass
2 encapsulant
3 cell
4 back sheet
5 interconnector

Figure 32 – Structure of c-Si PV module

Table 12 – Example of failure modes of PV module via materials

Interconnector broken	J-box failure	Bypass diode failure
Encapsulant: delamination, browning, loss of elastic, lower chemical bond		
Solder bond failure	Glass broken	Hot spot
Ground fault	Corrosion	Joint failure
Structural failure	Cell broken/Cell crack	Electric arc

7.3 Test methods

7.3.1 Crystalline silicon photovoltaic module type-approval international standard

IEC 61215-1 [23] specifies the requirements for design qualification verification and type approval for terrestrially installed photovoltaic modules suitable for long-term operation outdoors in typical weather conditions.

The objective of the series of tests performed in accordance with IEC 61215-1 is to determine the module's electrical and temperature characteristics and (as much as possible within time and cost constraints) to verify that the module can withstand long-term exposure to typical weather conditions [23]. The tests are intended to serve as screening tests designed to eliminate initial failures. Figure 33 shows the test sequence. For the damp heat test (DHT: 85 °C/85 % RH), IEC 60068-2-67 specifies a test time of 1 000 h, and actual test times of over 2 000 h have been suggested. For this research, the DHT was extended up to 4 000 h.

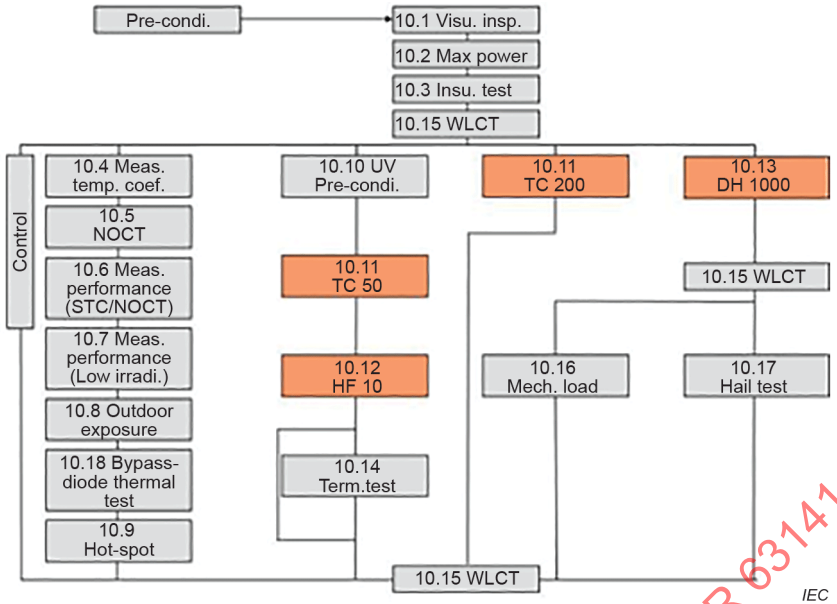

Figure 33 – Qualification test sequence in IEC 61215-1 [23]

7.3.2 Air-HAST work

HAST, highly-accelerated temperature and humidity stress test, is also called in IEC 60068-2-66 "Damp heat, steady state (unsaturated pressurized vapour)". In 1990, LED evaluation was reported with residual air left in the HAST chamber [4]. The air-containing HAST is referred to as "air-HAST". Moreover, air-HAST was used for whisker evaluations of lead-free semiconductor package solder mounting in 2010 [14].

For the research of this document, HAST and air-HAST were conducted to investigate whether the previous findings on these methods can be applied to accelerated testing of photovoltaic modules. The HAST and air-HAST conditions used are given below.

7.3.3 Test samples

Figure 34 shows the PV module (single-cell module of 18 cm × 18 cm) used for testing. Table 13 shows the component configuration. All the components were constructed with commercial products. Single-cell polycrystalline silicon was used, and the same glass and sealant were used throughout. Deterioration due to moisture permeation was categorized into three processes:

a) backsheet moisture penetration (moisture reaching the sealant),

b) sealant moisture penetration (sealant moisture penetration/diffusion speed prior to moisture reaching the cell),

c) progressive cell corrosion (corrosion progress speed/corrosion mode after moisture has reached the cell).

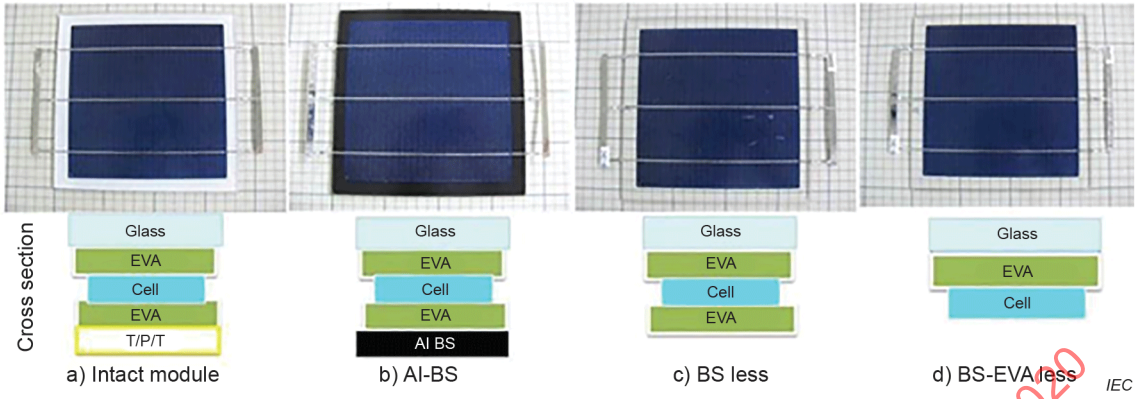

Figure 34 – Appearance of modules

Table 13 – Specifications of materials used in PV module

Material	Specification	Supplier[a]
Cell	Multicrystalline Si cell (156 mm × 156 mm)	Q Cells
Glass	Semi-tempered glass	AGC
Encapsulant	EVA (Fast cure)	SANVIC
Interconnector	A-SPS (Leaded, Ag)	Hitachi Cable
Back sheet	TPT/Al	Non-disclosure

[a] This information is given for the convenience of users of this document and does not constitute an endorsement by IEC of the companies named.

Samples with different back surface structures were created to investigate whether the progress of deterioration is different for each process type.

To investigate deterioration process a), backsheets with a PVF/PET/PVF (TPT) composition, which is a standard module structure (intact module), were created. Modules with backsheets having a PET/Al/PET composition were created to prevent moisture permeation from the back surface on a comparison.

To investigate deterioration process b), backsheet-free modules in which the backsheet had been omitted from the rear surface were created.

To investigate deterioration process c), backsheet/EVA-free modules in which the backsheet and EVA (ethylene vinyl acetate) normally used on the back surface had been omitted, were created.

None of the modules, which were created to investigate deterioration processes, had the four-sided frame made of aluminum or another metal that is present in commercial photovoltaic modules.

7.3.4 Test conditions

The PV modules were exposed to DHT conditions, 85 °C/85 % RH in an ESPEC PL-2KP chamber and were exposed to conditions over 100 °C and high humidity in an ESPEC EHS-211 HAST chamber. The test conditions are summarized in Table 14.

The DH test conditions in IEC 61215-1 is 85 °C for temperature, 85 % RH for humidity, 1 000 h for the testing time. In these test conditions, the testing time is extended to 4 000 h. The typical HAST humidity condition is 85 % RH with unsaturated vapour.

In Table 14, the conditions with saturated 100 % humidity and over 100 °C temperature are named "saturated HAST". The PV modules were exposed to 105 °C/100 % RH and 120 °C/100 % RH for "saturated HAST" conditions and 110 °C/85 % RH for HAST conditions.

Table 15 shows test conditions with the ratios of air-pressure to water-vapour pressure. The ratios of air-pressure to water-vapour pressure in DHT conditions are half-and-half whereas the HAST test condition is 100 % water-vapour pressure. So air-HAST is developed with water-vapour pressure and air-pressure in HAST temperature and humidity. In air-HAST, the test conditions are 110 °C/85 % RH with air-pressure, 0,128 MPa (in theoretical value) and air-pressure to water-vapour pressure is half-and-half. Air HAST is evaluated for an accelerated test containing air with oxygen to corrode and oxidize photovoltaic modules.

The specimens for each test time for air-HAST conditions are tested separately. Before starting and during the defined exposure periods, the characteristics of these PV modules were frequently evaluated to measure the current-voltage measurement (I-V measurement), to observe visual inspection and electroluminescence (EL) images. The ends of the electrodes of all modules are opened under environmental tests.

Table 14 – Test conditions

Test condition	Temperature/ humidity	Test time
Damp heat test	85 °C/85 % RH	4 000 h
HAST	105 °C/100 % RH	1 000 h
	110 °C/85 % RH	800 h
	120 °C/100 % RH	400 h
Air-HAST	110 °C/85 % RH	800 h

Table 15 – Test conditions and partial pressures

	Temperature (°C)	Humidity (% RH)	Water vapour partial pressure (MPa abs.)	Total pressure (MPa abs.)	Partial pressure of air (MPa abs.)
Room temperature	25	60	0,001 6	0,101 3	0,099 7
DH	85	85	0,049 5	0,101 0	0,051 8
HAST	105	100	0,120 8	0,120 8	0
	110	85	0,121 6	0,121 6	0
	120	100	0,198 5	0,198 5	0
Air-HAST	110	85	0,121 6	0,249 8	0,128 2

7.3.5 Measurement and analysis

7.3.5.1 I-V measurement

I-V measurement is a method of measuring current while varying the bias voltage, then plotting the data obtained to create an I-V curve. The current when the voltage is 0 V is called the short current (I_{sc}). The voltage when no current is flowing in the photovoltaic cell is called the open-circuit voltage (U_{oc}). To extract the maximum power from the photovoltaic cell, it should be operated at the point at which the product of the voltage and current is the maximum. This point is called the maximum power (P_{max}).

7.3.5.2 EL measurement

EL measurement is a measurement method in which a bias current is applied to a photovoltaic module in the forward direction to generate a phenomenon known as electroluminescence (EL) from the PN junctions. This electroluminescence is detected and imaged to enable visualization of problems such as cell cracks and finger electrode wire breaks, which are difficult to see in optical images. Dark I-V measurements are invaluable in examining the diode properties (series resistance, parallel resistance, saturation current under backward voltage).

7.3.5.3 Dark I-V measurement

In the dark, photovoltaic cells act as large flat diodes. Their diode characteristic can be evaluated directly by applying a reverse bias in the dark and measuring the I-V characteristic. This measurement is known as dark I-V measurement. By measuring the diode breakdown characteristic and internal resistance values, it is possible to see the changes in the series and parallel resistance components.

7.3.5.4 Ion chromatography

Ion chromatography is an analysis method that separates and quantifies ions by using differences in ion adsorption rates relative to an ion exchange resin. It can be used to analyse the concentrations of various ions in liquid samples at sensitivities as high as a few parts per billion.

7.4 Test results

7.4.1 DHT testing

Figure 35 compares typical EL images of DHT test samples in the test time ranging from 0 h to 4 000 h under the conditions of 85 °C/85 % RH. Figure 36 shows the change of the P_{max} value of each sample, expressed as a ratio of the initial value.

As the test time increased, each sample's P_{max} value decreased relative to its initial value. The rates by which P_{max} had decreased after a test time of 3 000 h were roughly the same for all the sample types, under 10 %(except the Al-BS one sample).

Starting at the 3 500 h-mark, P_{max} dropped drastically for the intact module samples and aluminum backsheet samples. At the 4 000 h-mark, the decrease in P_{max} relative to the initial value was 57 % for the intact module samples, and 15 % to 20 % for the aluminum backsheet samples.

The EL image for the intact module and Al-BS_3 shown in Figure 35 indicates that the sample's brightness had become unbalanced, and as shown in Figure 36, its P_{max} value had decreased by 50 %. It can be deduced that these results are caused by interconnector breakage and decreasing output during measurement.

The P_{max} value of the backsheet-free samples, on the other hand, dropped moderately. It decreased by 7 % after a test time of 4 000 h, which was about the same as the decrease after 3 000 h.

The intact module samples showed the appearance of small dark areas at cell edges in the EL images for test times of up to 3 000 h, but were almost unchanged. Starting at the 3 500 h-mark, the dark areas in the EL images of the intact module samples started growing from the cell edges to the cell interior, and they had grown close to the cell centre by the 4 000 h-mark.

The EL images of the aluminum backsheet samples showed dark areas appearing from the cell edges starting at the 3 500 h-mark, but they had not progressed from the cell edges even by the 4 000 h-mark. The backsheet-free and backsheet/EVA-free samples showed the appearance of some dark areas along interconnectors, but were almost unchanged.

Figure 35 – EL images after DHT

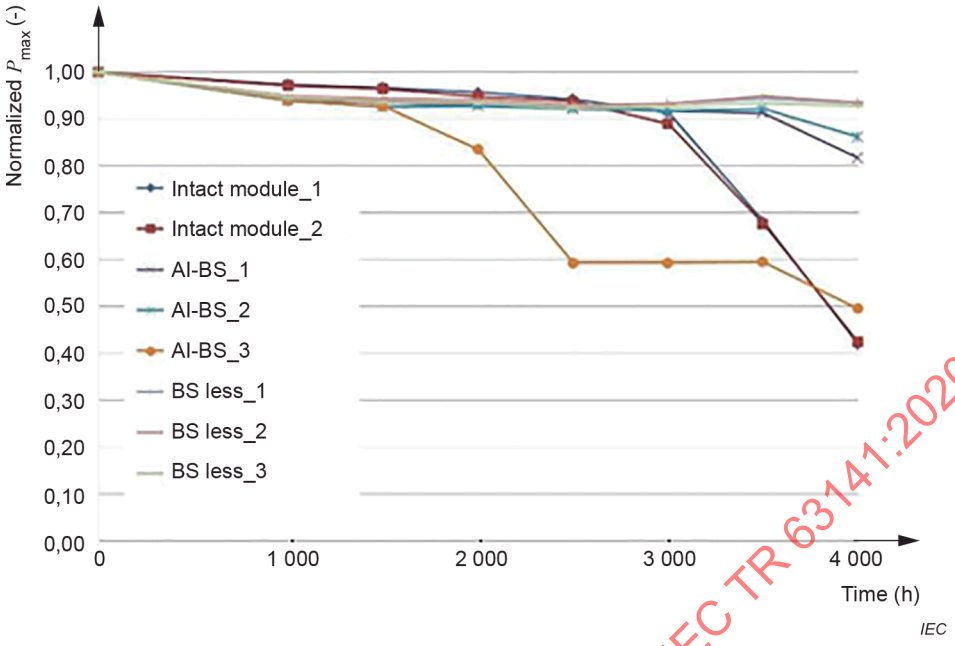

Figure 36 – Degradation profiles with DHT

7.4.2 Saturated HAST

Figure 37 shows the EL images of saturated HAST samples at conditions of 105 °C/100 % RH after a test time of 1 000 h. Figure 38 compares the EL images of HAST samples at conditions of 120 °C/100 % RH with test times of 0 h and 400 h. Figure 39 shows the P_{max} values of the samples, each expressed as a ratio of the initial value.

Only the intact module samples were subjected to test conditions of 105 °C/100 % RH for 1 000 h. The P_{max} value of these samples showed a decrease of 10 % at the 500 h-mark, followed by a moderate change toward the 1 000 h-mark.

The EL images of these samples showed dark areas between finger electrodes. Under test conditions of 120 °C/100 % RH for 400 h, the P_{max} value decreased by 16 % for the intact module samples, 37 % for the aluminum backsheet samples, 2 % for the backsheet-free samples, and 17 % for the backsheet/EVA-free samples. The EL images of the intact module and aluminum backsheet samples showed dark areas growing from the edges. The EL images of the backsheet-free samples showed dark areas growing from the cell centre.

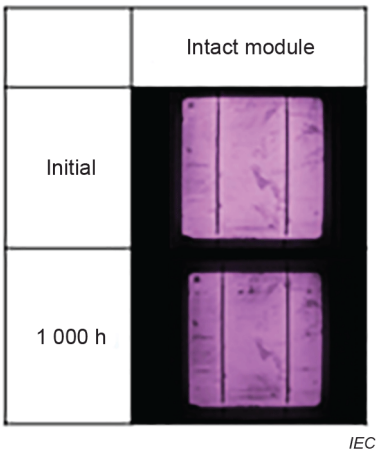

Figure 37 – EL images of HAST 105 °C/100 % RH